WL-TR-94-4006

# EDDY CURRENT FOR DETECTING SECOND LAYER CRACKS UNDER INSTALLED FASTENERS



WILLIAM R. SHEPPARD

NORTHROP CORPORATION
B-2 DIVISION
8900 E. WASHINGTON BLVD.
PICO RIVERA CA. 90660

APRIL 1994

FINAL REPORT FOR 10/01/91 - 11/01/93



APPROVED FOR PUBLIC RELEASE; DISTRIBUTION IS UNLIMITED.



MATERIALS DIRECTORATE
WRIGHT LABORATORY
AIR FORCE MATERIEL COMMAND
WRIGHT PATTERSON AFB OH 45433-7734

# NOTICE

When Government drawings, specifications, or other data are used for any other purpose other than in connection with a definitely Government-related procurement, the United States Government incurs no responsibility or any obligation whatsoever. The fact that the government may have formulated or in any way supplied the said drawings, specifications, or other data, is not to be regarded by implication, or otherwise in any manner construed, as licensing the holder, or any other person or corporation: or as conveying any rights or permission to manufacture, use, or sell any patented invention that may be related thereto.

This report is releasable to the National Technical Information Service (NTIS). At NTIS, it will be available to the general public, including foreign nations.

This technical report has been reviewed and is approved for publication.

GREGORY M. JABLUNOVSKY, Capt, USAF
Nondestructive Evaluation Branch
Metals and Ceramics Division

TOBEY M. CORDELL, Chief
Nondestructive Evaluation Branch
Metals and Ceramics Division

FOR THE COMMANDER

NORMAN M. GEYER, Acting Chief
Metals and Ceramics Division
Materials Directorate

If your address has changed, if you wish to be removed from our mailing list, or if the addressee is no longer employed by your organization please notify WL/MLLP Bldg 655, 2230 Tenth St Ste 1, WPAFB, OH 45433-7817 to help us maintain a current mailing list.

Copies of this report should not be returned unless return is required by security considerations, contractual obligations, or notice on a specific document.

# REPORT DOCUMENT PAGE

*Form Approved*
*OMB No. 0704-0188*



| 1. AGENCY USE ONLY *(LEAVE BLANK)* | 2. REPORT DATE | 3. REPORT TYPE AND DATES COVERED |
|---|---|---|
| | APRIL 1994 | FINAL 10/01/91--11/01/93 |

**4. TITLE AND SUBTITLE**

EDDY CURRENT FOR DETECTING SECOND LAYER CRACKS UNDER INSTALLED FASTENERS

**5. FUNDING NUMBERS**

C F33615-91-C-5660
PE 62102
PR 2418
TA 02
WU 52

**6. AUTHOR(S)**

WILLIAM R. SHEPPARD

**7. PERFORMING ORGANIZATION NAME(S) AND ADDRESS(ES)**

NORTHROP CORPORATION
B-2 DIVISION
8900 E. WASHINGTON BLVD.
PICO RIVERA CA 90660

**8. PERFORMING ORGANIZATION REPORT NUMBER**

**9. SPONSORING/MONITORING AGENCY NAME(S) AND ADDRESS(ES)**

MATERIALS DIRECTORATE
WRIGHT LABORATORY
AIR FORCE MATERIAL COMMAND
WRIGHT PATTERSON AFB OH 45433-7734

**10. SPONSORING/MONITORING AGENCY REPORT NUMBER**

WL-TR-94-4006

**11. SUPPLEMENTARY NOTES**

**12a. DISTRIBUTION/AVAILABILITY STATEMENT**

APPROVED FOR PUBLIC RELEASE;
DISTRIBUTION IS UNLIMITED.

**12b. DISTRIBUTION CODE**

**13. ABSTRACT** *(MAXIMUM 200 WORDS)*

The detection of second layer Cracks Under Fasteners (CUF) persists as an Air Force Logistics need. This work seeks to extend technology developed for detecting cracks in aluminum alloy substructure below graphite-epoxy skins, to structures with an aluminum first layer. Improvements to the design of the Northrop Low Frequency Eddy Current Array (LFECA) system are identified to improve sensitivity to CUFs in aluminum-over-aluminum structures. The probe core shape, dimensions, and coil configurations were optimized for detection with installed fasteners and metallic skin. A multiparameter analysis algorithm is applied to enable flaw discrimination from centering variations, edge responses and other sources of noise. The study also quantifies the capabilities and limitations of the LFECA system.

**14. SUBJECT TERMS**

EDDY CURRENT, LOW FREQUNCY EDDY CURRENT, CRACKS, CUFS, NONDESTRUCTIVE EVALUATION (NDE)

**15. NUMBER OF PAGES**

60

**16. PRICE CODE**

| 17. SECURITY CLASSIFICATION OF REPORT | 18. SECURITY CLASSIFICATION OF THIS PAGE | 19. SECURITY CLASSIFICATION OF ABSTRACT | 20. LIMITATION OF ABSTRACT |
|---|---|---|---|
| UNCLASSIFIED | UNCLASSIFIED | UNCLASSIFIED | UL |

FORMS DISK

## FOREWORD

This Final Technical Report covers the work performed from 30 October 1991 to 30 November 1993 under contract F33615-91-C-5660 entitled "Eddy Current for Detecting Second Layer Cracks Under Installed Fasteners." The report was prepared by the Northrop Corporation, B-2 Division, Pico Rivera, California. The contract was administered under the technical direction of Capt. Greg Jablunovsky (WL/MLLP), Nondestructive Evaluation Branch, Wright-Patterson Air Force Base, Ohio. Claudia Kropas was the Air Force Project Engineer prior to Capt. Jablunovsky.

Northrop Corporation, B-2 Division served as the prime contractor with Mr. William Sheppard as program manager and principal investigator. He was assisted by Mr. Owen Manning in the design evaluation task. Dr. Floyd Spencer and Mr. David Moore of Sandia National Laboratories provided access to the FAA sponsored Aging Aircraft NDI Validation Center and performed as monitors on the validation exercise.

## CONTENTS

## ILLUSTRATIONS

## ILLUSTRATIONS(Continued)

## ILLUSTRATIONS(Continued)

# SECTION 1

# INTRODUCTION

All military aircraft structures use skins fastened to substructures. This design results in thousands of fastener holes and hidden structure. As fatigue cracks frequently initiate at fastener holes, inspecting the area immediately around the hole (and under the fastener head) is critical to the flight safety of the airframe.

Unfortunately, the existing inspection methods used to detect second layer cracks under fasteners (CUFs) either requires fastener removal or are lacking in the requisite sensitivity. Fastener removal is generally a difficult and expensive task which can itself result in damage to the structure and is undesirable as a prerequisite to inspection. Other existing inspection methods which can detect second layer cracks without removing the fastener, such as radiography and conventional eddy current, will detect cracks only after they have grown to a size which is costly or difficult to repair.

A need was identified by Northrop in 1989 for improved CUF detection on the F/A-18 vertical stabilizers. CUFs were occurring in the vertical stabilizer aluminum spars which are fastened under composite skins by titanium fasteners. A sensitive inspection system was needed to detect CUFs in the aluminum spars with the skins and fasteners installed. For this reason, an updated/modified low frequency eddy current array (LFECA) system was designed and constructed in 1990 by Northrop.[1] The design of this system was based on previous research and development work performed under Air Force contracts and Northrop independent research and development efforts.[2,3] The LFECA system was successfully demonstrated as a sensitive CUF detection system for the F/A-18 vertical stabilizer inspection.

This program was to develop the design modifications required to make the LFECA system a sensitive second layer CUF detection system for airframe structures constructed of aluminum skins with aluminum substructures.

## 1.1 PROGRAM OBJECTIVE

The overall objective of this program was to design an eddy current inspection system to detect cracking in the second layer of fastened aluminum aircraft structures without requiring the removal of fasteners.

## 1.2 PROGRAM APPROACH

This program defined the improvements to the Northrop LFECA design required to achieve maximum sensitivity to CUFs in aircraft structures with aluminum skins and substructures. This work was conducted in three tasks.

### 1.2.1 TASK I - BREADBOARD DESIGN

In this task, the hardware improvements to the LFECA design required to conduct an eddy current inspection on second layer structures were defined. A major portion of this task was focused on optimizing the LFECA probe design. Variations in probe design were evaluated to determine their impact on the sensitivity to CUFs, structure ,and probe placement. These evaluations essentially determined the effect of probe design on the generation of an eddy current field and the detection of perturbations in the field surrounding a fastener hole. Special consideration was given in the probe design to the ability to compensate for the probe's response to nonrelevant features such as adjacent structure and probe placement. The results of these evaluations allow for the design of an optimum LFECA probe for specific or general applications.

### 1.2.2 TASK II - ALGORITHM DEVELOPMENT

In this task, software algorithms were developed which remove or isolate unwanted probe responses from the CUF response. Responses caused by structure and probe placement are two examples of sources for unwanted probe responses. The unique features of the LFECA probe design, such as multiple drive coils and sense coil arrays, are used in combination with a multiparameter analysis method to form the compensation algorithms.

### 1.2.3 TASK III - DESIGN EVALUATION

In this task, the LFECA system design improvements developed in *Tasks I and II* are evaluated. A description of the effectiveness of these improvements is reported.

# SECTION 2

# TASK I - BREADBOARD DESIGN

In this task, the hardware improvements to the LFECA probe and system design required to conduct an eddy current inspection of second layer aluminum aircraft structures were defined. A series of analytical and experimental evaluations were performed to define the optimum design solutions. Optimizing the LFECA probe design constituted the majority of effort in this task. The results from this task were used in Task II for algorithm development and in Task III for design evaluation.

## 2.1 PROBE DESIGN

A system capable of measuring the three dimensional magnetic field profiles of potential LFECA probe configurations was developed for use in this program. This system was used to perform a series of experimental evaluations to establish a background for designing improved LFECA probes and compensation algorithms. The basic goal was to improve CUF sensitivity and improve the ability to compensate for nonCUF related responses. A summary of the most salient results of these evaluations and their relationship to improving the LFECA system design will be presented.

### 2.1.1 Sense Coil Optimization

The current LFECA probe design uses the sense coils to detect the normal magnetic field component present at the outer rim of the probe core. A series of measurements were performed to evaluate the benefit of altering the sense coil arrangement and/or the magnetic field component sensed. In these measurements the transverse and normal magnetic field components present at the face of the probe were measured under different probe and specimen conditions.

Figure 1 shows a sketch of the experimental setup used to measure the magnetic fields present at the probe face as the probe drive coil is energized. A slender magnetic field sensor is inserted between the probe face and an aluminum test specimen. A gap of 2 mm (0.08-inch) is required between the probe and the test specimen. An x-y-z scanning bridge is attached to the sensor enabling the mapping of the fields across the probe face. Depending on sensor orientation, the sensor can detect either the normal or transverse magnetic field component. One, two, and three dimensional field maps have been constructed from measurements; however, only one dimensional (single line) scans are presented in this report. The magnetic field maps are stored on floppy disk and can be used as a reference to produce a map of the difference between two test specimens. For example, the difference between a specimen with and without a CUF can be shown to demonstrate the effect of a CUF.

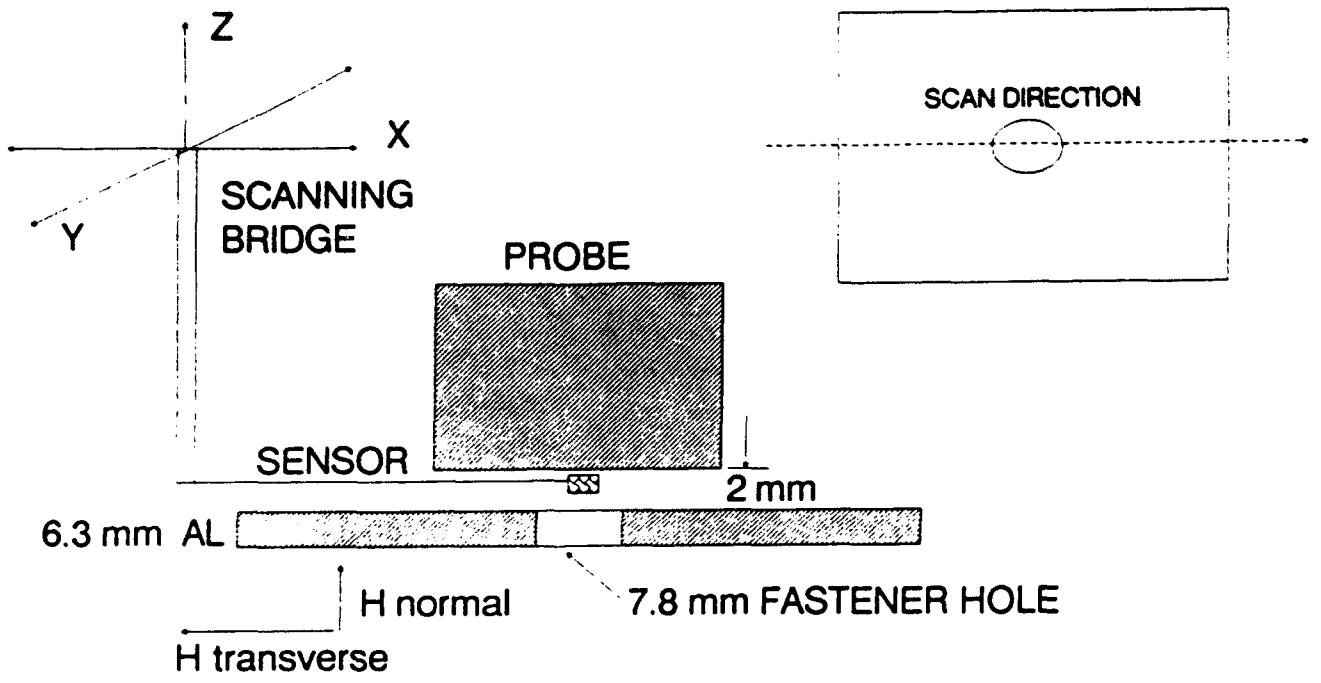


**FIGURE 1. MAGNETIC FIELD MEASUREMENT SET-UP.**

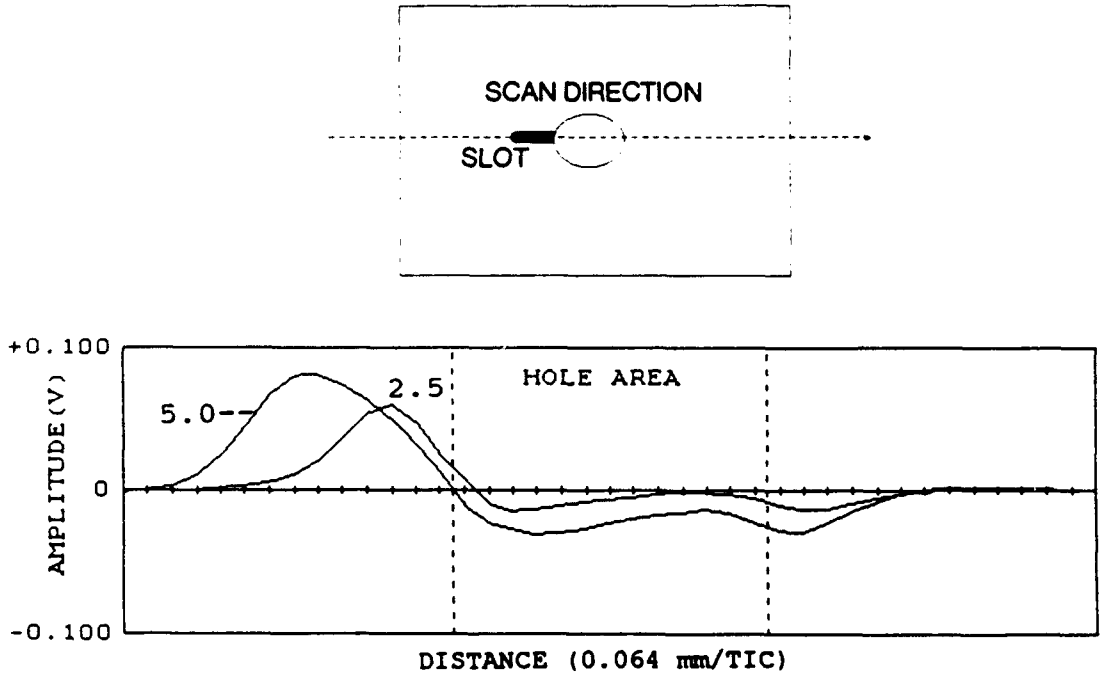


**FIGURE 2. NORMAL MAGNETIC FIELD COMPONENT AMPLITUDES AT THE PROBE FACE DUE TO A 2.5 mm SLOT AND A 5.0 mm SLOT USING A 10 kHz INSPECTION FREQUENCY.**

**CUF Response**

The LFECA probe detects a CUF by sensing the change in eddy current distribution caused by the CUF. A LFECA probe centered on a hole creates a distribution of eddy currents around the hole. A CUF disrupts these currents causing them to divert from the region around the hole at the crack site. If the eddy current distribution of a hole with a CUF were compared to the distribution without a CUF, the difference between these distributions would be a current which encircles the CUF. Therefore, the fields caused by a CUF can be modeled as a current loop which encircles the CUF. The shape and size of the current loop are determined by the CUF size and inspection frequency. A larger CUF results in a larger sized loop. At high frequencies the current loop flows closely around the CUF and as the inspection frequency is decreased the current loop spreads out in a radial direction from the CUF.

Figure 2 shows the normal magnetic field component due to a 2.5 mm (0.1-inch) and a 5.0 mm (0.2-inch) through slot radiating from the fastener hole. Using the setup shown in Figure 1, this measurement was taken by scanning the sensor in a line which ran lengthwise along the CUF and through the center of the fastener hole. A specimen without a slot was scanned as a reference and the eddy current field response was subtracted from that for specimens with slots to obtain the slot responses. Each of the specimens had 7.8 mm (0.312-inch) holes. Fasteners were not installed for the scans. The experimental procedure is a good approximation for titanium or stainless steel fasteners which have a permeability of 1 and low conductivity. In Figure 2 the peak response of the fields occurs a little more than halfway along the slot length. This is compatible with the model of a current loop encircling the CUF.

Figure 2 showed the distribution of fields to be expected at high frequencies (10 kHz) because of a near surface CUF. Figure 3 shows a scan of the 2.5 mm (0.1-inch) slot at 10 kHz (as shown in Figure 2) and at 600 Hz. A reduction in frequency causes a spreading of the fields in a radial direction away from the slot and a drift in the peak away from the hole ( to over the slot tip). Figure 4 shows a scan across the width of the 2.5 mm (0.1-inch) slot at 10 kHz and at 600 Hz. The fields spread in the same manner as they move beyond the slot tip, as seen in Figure 3.

The change in current distribution with frequency can be easily visualized by observing the changes in the transverse magnetic field component. The distribution of this component resembles the eddy current distribution. Figure 5 shows the transverse magnetic fields (field component in slot length direction) from a 5 mm (0.2-inch) slot at 10 kHz and 600 Hz. The high frequency response (10 kHz) shows the positive and negative cycles that would be expected from a scan across a loop of current tightly encircling the slot. The low frequency response (600 Hz) has the same shape near the fastener hole but does not have a companion peak beyond the crack tip. The fields spread beyond the crack tip, as is indicated by the outward drift of the normal magnetic field component peak (shown in Figure 3) into the material. The fields (eddy currents) at the edge of the hole do not spread because of the boundary imposed by the walls of the fastener hole.

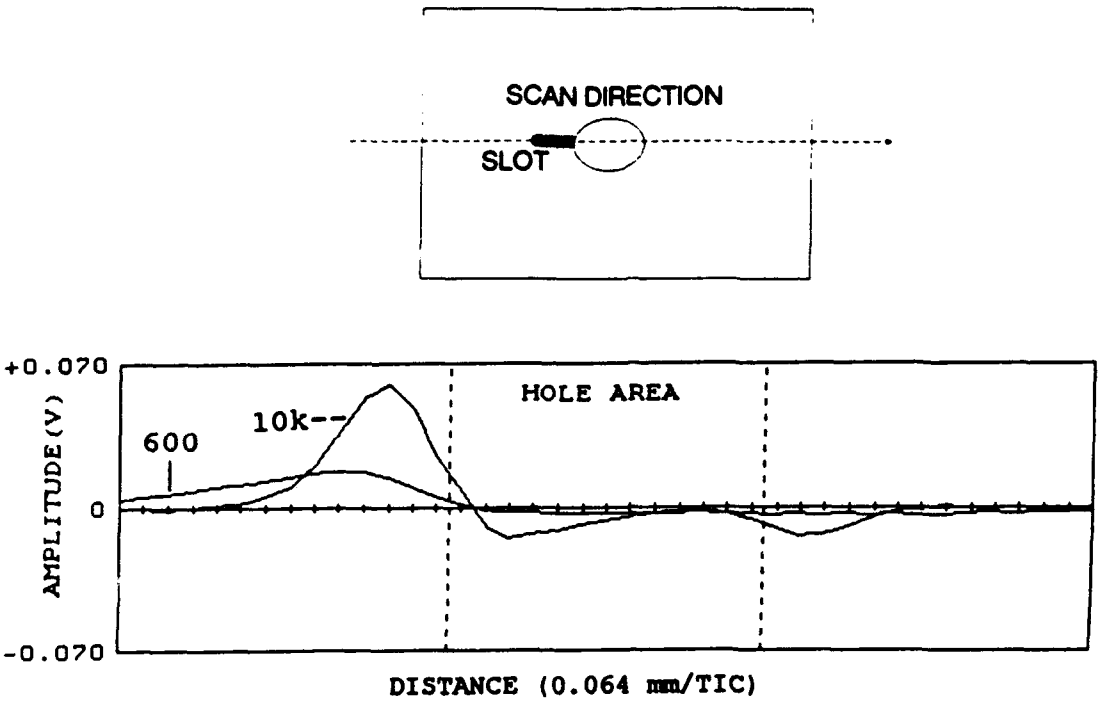


**FIGURE 3. NORMAL MAGNETIC FIELD COMPONENT AMPLITUDES AT 10 kHz AND AT 600 Hz DUE TO A 2.5 mm SLOT.**

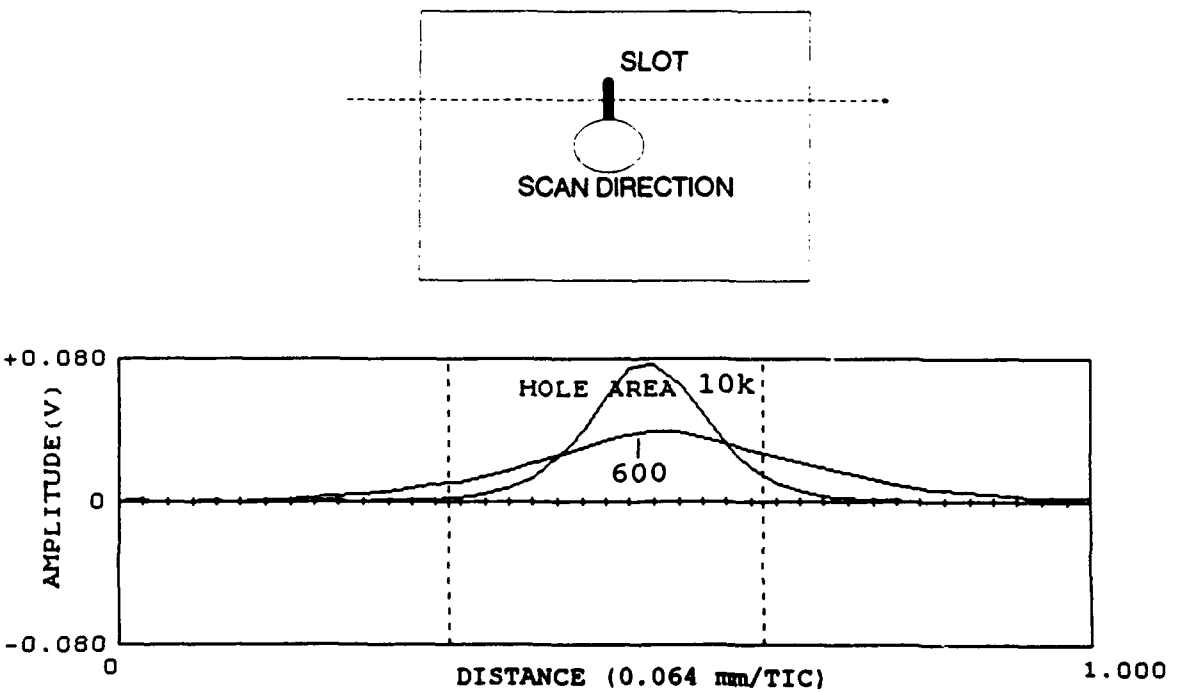


**FIGURE 4. NORMAL MAGNETIC FIELD COMPONENT AT 10 kHz AND 600 Hz DUE TO A 2.5 mm SLOT WHEN SCANNED ACROSS THE WIDTH OF THE SLOT.**

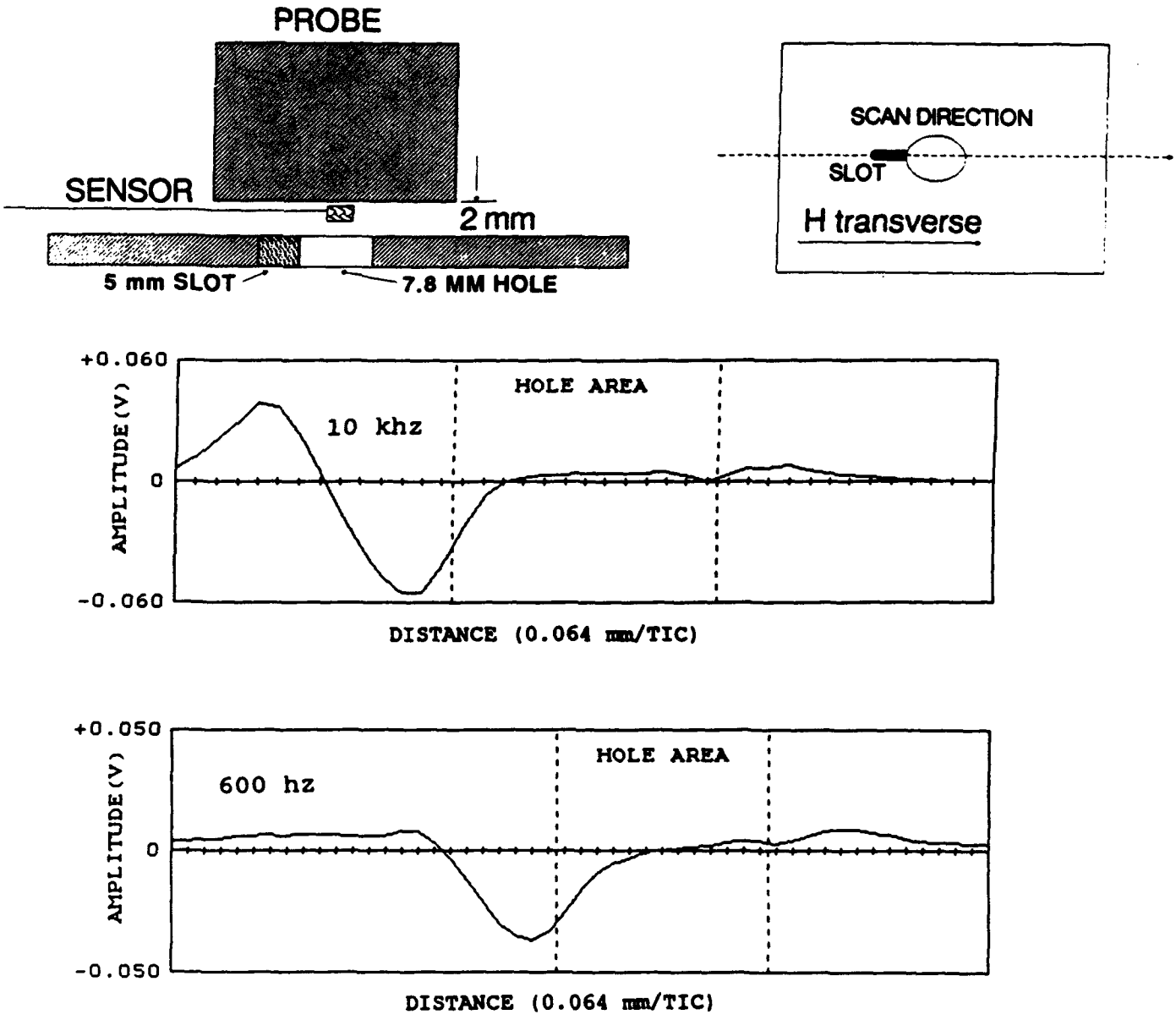


**FIGURE 5. TRANSVERSE MAGNETIC FIELD COMPONENTS AT 10 kHz (TOP) AND AT 600 Hz (BOTTOM) DUE TO A 5.0 mm SLOT. HORIZONTAL SCALES ARE DIFFERENT TO SHOW RADIAL SPREAD AT LOW FREQUENCIES.**

All the responses shown so far have been from near surface defects. The response from a CUF residing in the second layer under an aluminum skin can also be modeled using the current loop analogy. Two additional effects need to be considered to understand the fields originating from a second layer CUF. These are (1) shielding of the second layer by the aluminum skin and (2) the increased distance from the probe face to the second layer.

Shielding by the aluminum skin decreases the magnetic field strength penetrating the second layer thereby reducing the strength of the eddy currents induced in the second layer. Shielding also reduces the fields radiated by the eddy current loop around the CUF. The result is a significant reduction in magnetic field strength measured at the probe face. The degree of reduction is frequency dependent following the skin depth relationship. Shielding also causes the field distribution to be narrowed to more directly over the CUF/current loop (this is a minor effect). In addition to the magnitude reduction, the fields are delayed (phase shifted) dependent on the frequency (delay is in proportion to thickness/skin depth).

The increased distance between the probe face and the second layer results in a reduced magnetic field magnitude as well as weaker eddy currents in the second layer. This occurs because of the probe drive coil geometry. At low frequencies the reduction in field strength due to drive coil geometry usually predominates over reductions caused by the shielding effect of the aluminum skin. An increased distance also results in a spreading of the fields radiating from the currents looping around the CUF. Figure 6 shows a scan of the normal magnetic field component resulting from a 5 mm (0.2-inch) slot with minimum (2 mm or 0.08-inch) and increased (6.3 mm or 0.25-inch) distance from the probe face to the test specimen. Increased lift-off also causes the fields to spread in a radial direction away from the CUF. This is the same effect that is observed as the distance (on axis) from a current loop is increased and closely follows analytic predictions.

Based on these measurements, it appears that moving the sense coils closer to the fastener hole could help improve CUF sensitivity. Improvements in CUF sensitivity would also be at the expense of sensitivity to adjacent structure. The exact placement of the sense coils is a compromise between CUF and adjacent structure sensitivity. If a sense coil sensitive to the normal magnetic field component is used, it should be placed as near to the center as possible to reduce adjacent structure sensitivity. Placing the sense coil closer to the center will achieve a greater sensitivity to small CUFs; however, this arrangement will also reduce the sensitivity to larger and second layer CUFs. Concentric sense coil arrays may be a useful approach to optimizing sensitivity to small and large CUFs. This arrangement would also provide more information on adjacent structure. Another option would be to enlarge the sense coils in the radial direction. This would increase the area of sensitivity and provide information from a larger area of the CUF fields.

Using a sensor which is sensitive to the transverse magnetic field component rather than the normal magnetic field component may not be as attractive as originally thought.

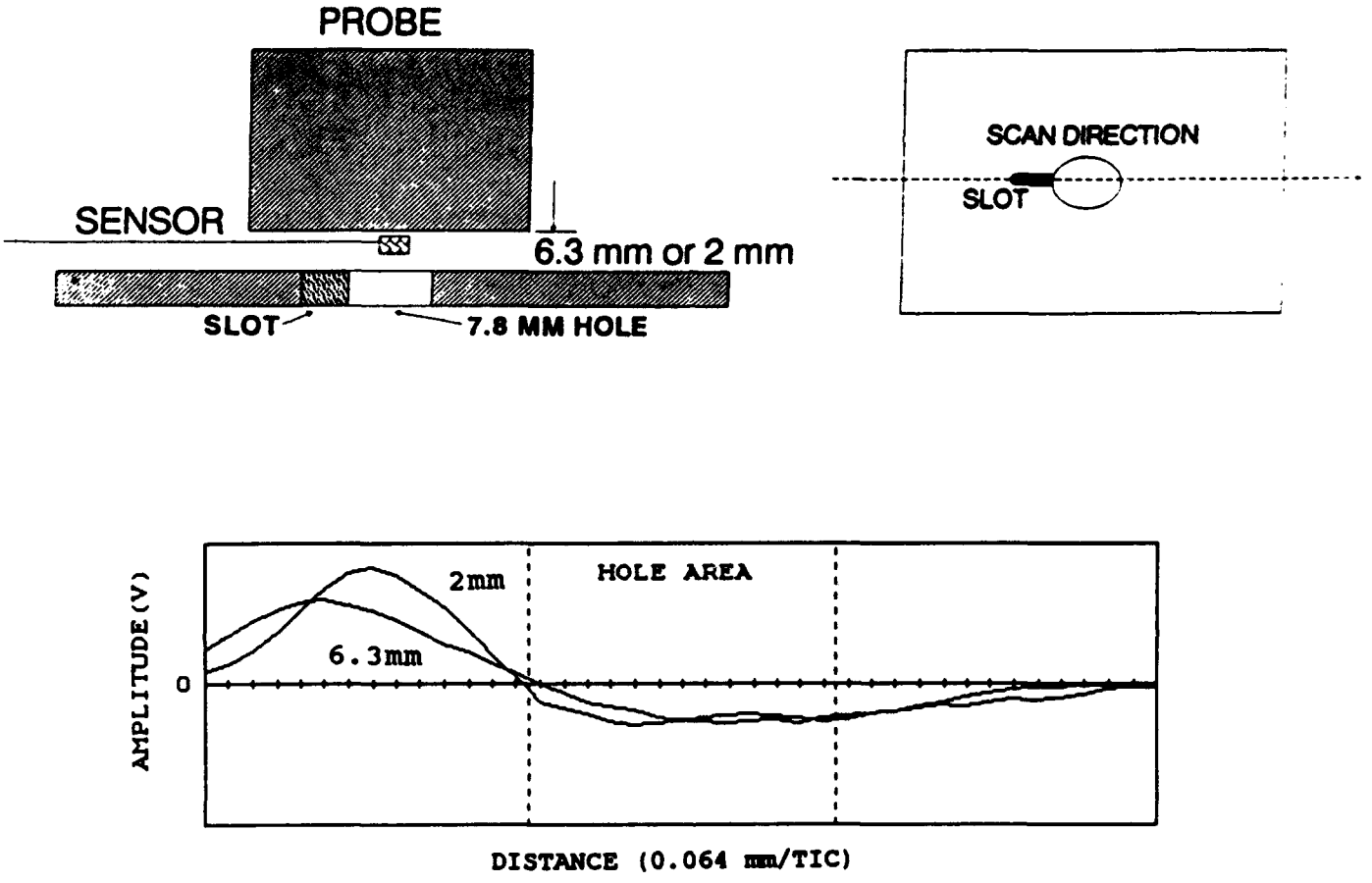


**FIGURE 6. NORMAL MAGNETIC FIELD DUE TO A 5 mm SLOT WITH A 2 mm AND A 6.3 mm SPACING BETWEEN THE PROBE FACE AND THE SPECIMEN.**

First, the magnitude of the transverse magnetic field component is usually two to three times smaller than the normal magnetic field component. This was determined from both analytical calculations and experimental measurements. Secondly, integrating a sense coil which is on its side into the LFECA probe imposes some practical difficulties. However, the transverse magnetic fields close to the fastener hole (due to the eddy currents against the fastener hole) could be a viable region of interest (see Figure 5). Detecting these fields would have some advantage in that they are close to the fastener hole and would have little sensitivity to adjacent structure. This field component would also be more proportional to CUF size and more sensitive to the fastener hole.

**Off-Center Response**

A series of measurements were performed to demonstrate the magnetic field perturbations caused by off-centering the probe. Figure 7 shows a series of scans measuring the normal magnetic field component at increasing off-center distances (0.2 to 1.0 mm). The off-center responses are linearly proportional to the off- center distance and agree with observations made in the past using the LFECA probe. The field distribution is indicative of having two current loops; one loop on each side of the hole each with opposite current directions. The loop shape is a rounded crescent which conforms to the fastener hole. The two- dimensional fields from the off-center scan differ from the CUF field response. This occurs because the current loop caused by the CUF conforms to the CUF while the off-center currents conform to the hole. The sense coil array could be configured to optimize its ability to detect the difference in spatial distribution between a CUF and other features. In addition to spatial differences between off-center and CUF responses, there is a difference in the phase response. At lower frequencies, see Figure 8, the fields due to an off-center condition spread out more in the radial direction but maintain a linear relationship between field magnitude and off-center distance.

**Edge Response**

The effect of an adjacent edge on the fields can be modeled by a loop of current aligned along the edge. The fields generated by this perturbation have different phase and two dimensional features than the field produced by a CUF. Figure 9 shows a series of scans of the normal magnetic field component across three specimens each with different hole to edge distances ( 15, 12 & 9 mm hole center to edge distances). The specimen-to-probe face distance was 6.3 mm (0.25-inch) to produce results similar to a second layer edge response. The fields spread away from the edge and interfere with those originating at the fastener hole. However, these fields have a different phase angle and spatial distribution from the fields originating at the fastener hole.

**Steel Fastener Response**

The data presented thus far are representative of the response anticipated from a structure fastened with a titanium, stainless steel (nonferromagnetic) or aluminum fastener. A steel (ferromagnetic) fastener introduces an additional factor which determines the fields near the fastener hole. Approximately eight times more current is generated in a ferromagnetic steel fastener head and shank than in an aluminum fastener. Figure 10 shows a comparison of the magnitudes of the transverse magnetic field components at 600

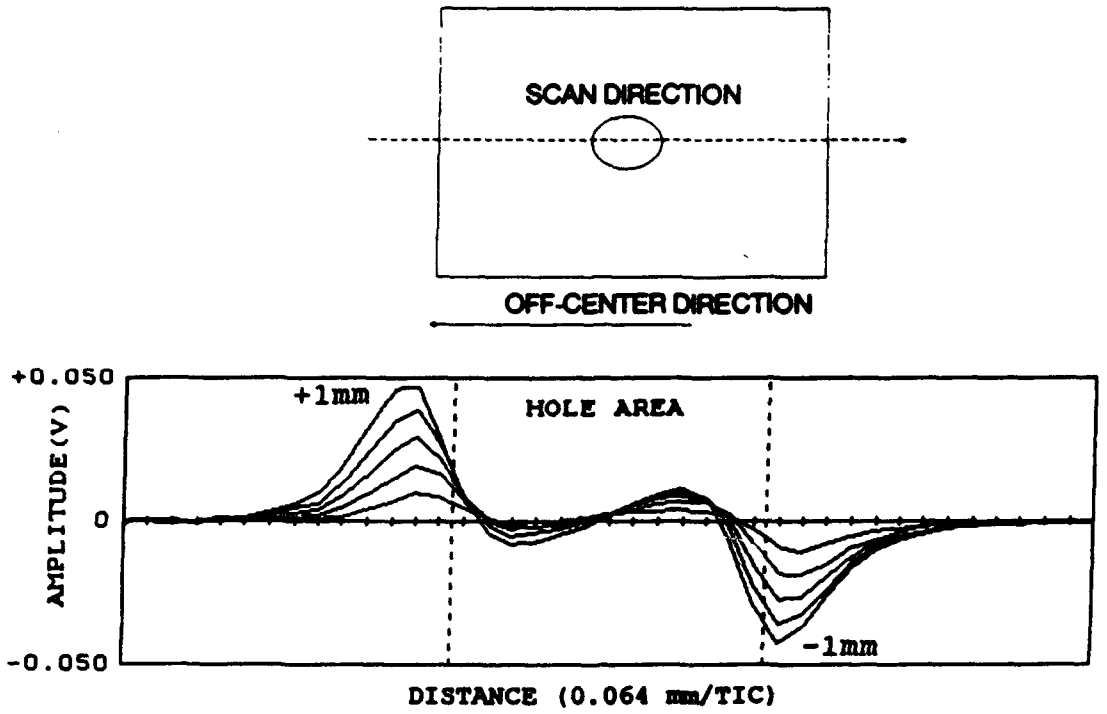


**FIGURE 7. NORMAL MAGNETIC FIELD COMPONENT DUE TO OFF-CENTER AT 10 kHz. SCANS AT 0.2, 0.4, 0.6, 0.8 AND 1.0 mm OFF-CENTER DISTANCES.**

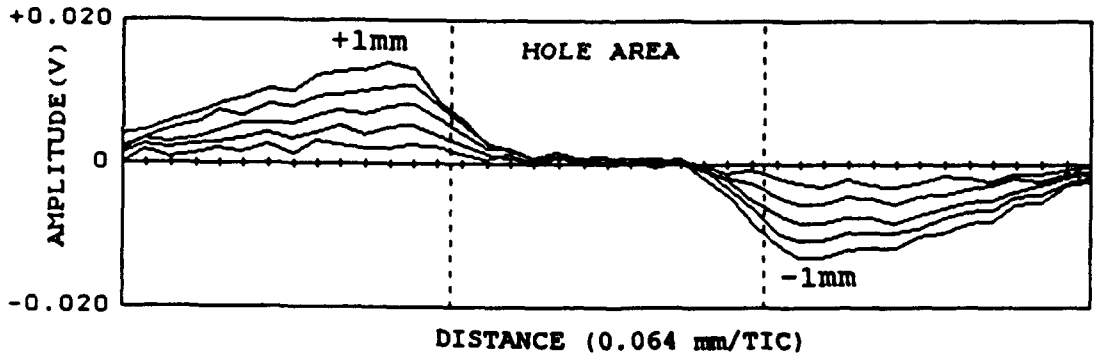


**FIGURE 8. NORMAL MAGNETIC FIELD COMPONENT DUE TO OFF-CENTER AT 600 Hz. SCANS AT 0.2, 0.4, 0.6, 0.8 AND 1.0 mm OFF-CENTER DISTANCES.**

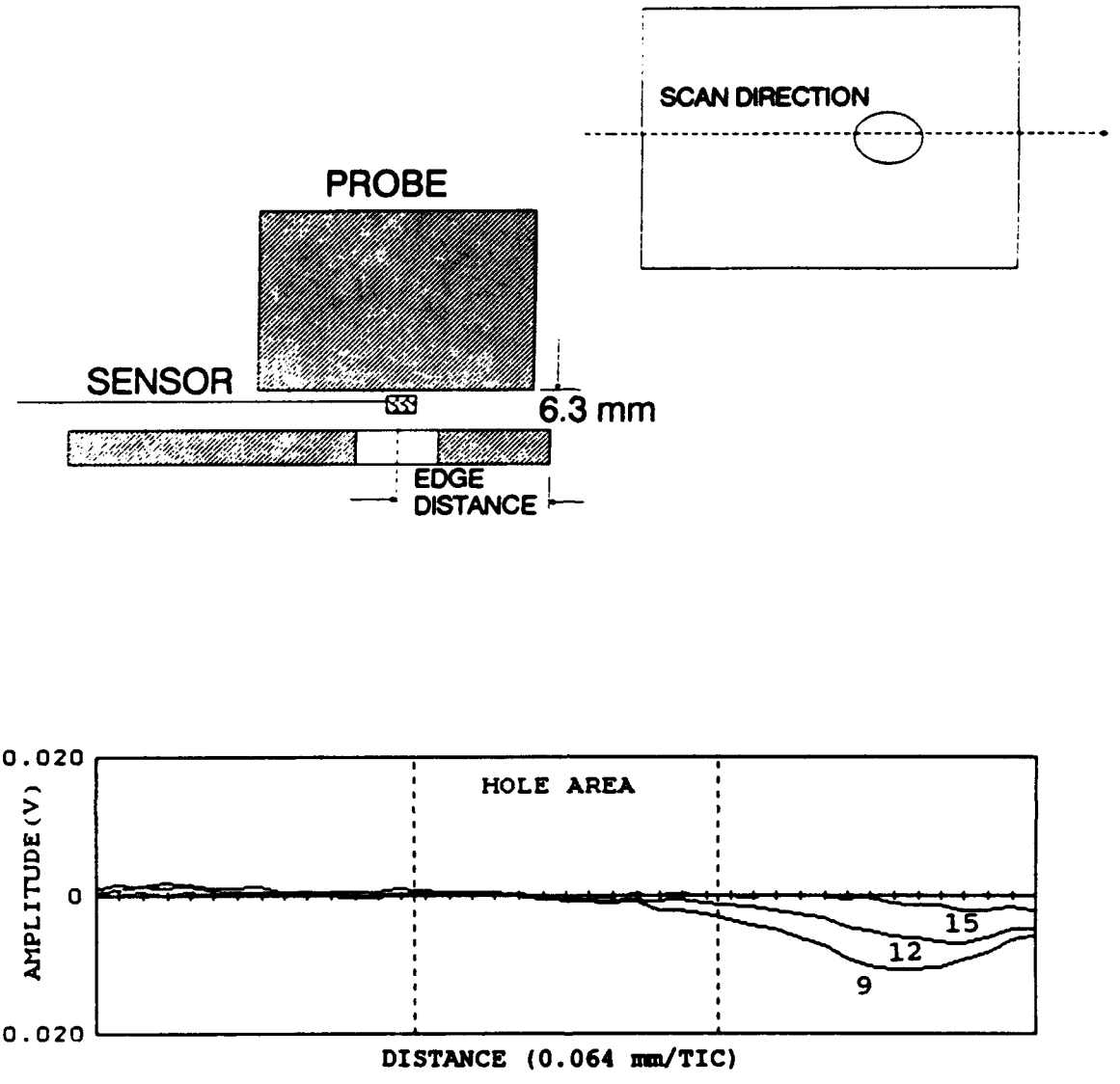


**FIGURE 9. NORMAL MAGNETIC FIELD COMPONENT DUE TO DIFFERENT EDGE TO HOLE DISTANCES. HOLE CENTER LINE TO EDGE DISTANCES OF 9, 12, AND 15 mm.**

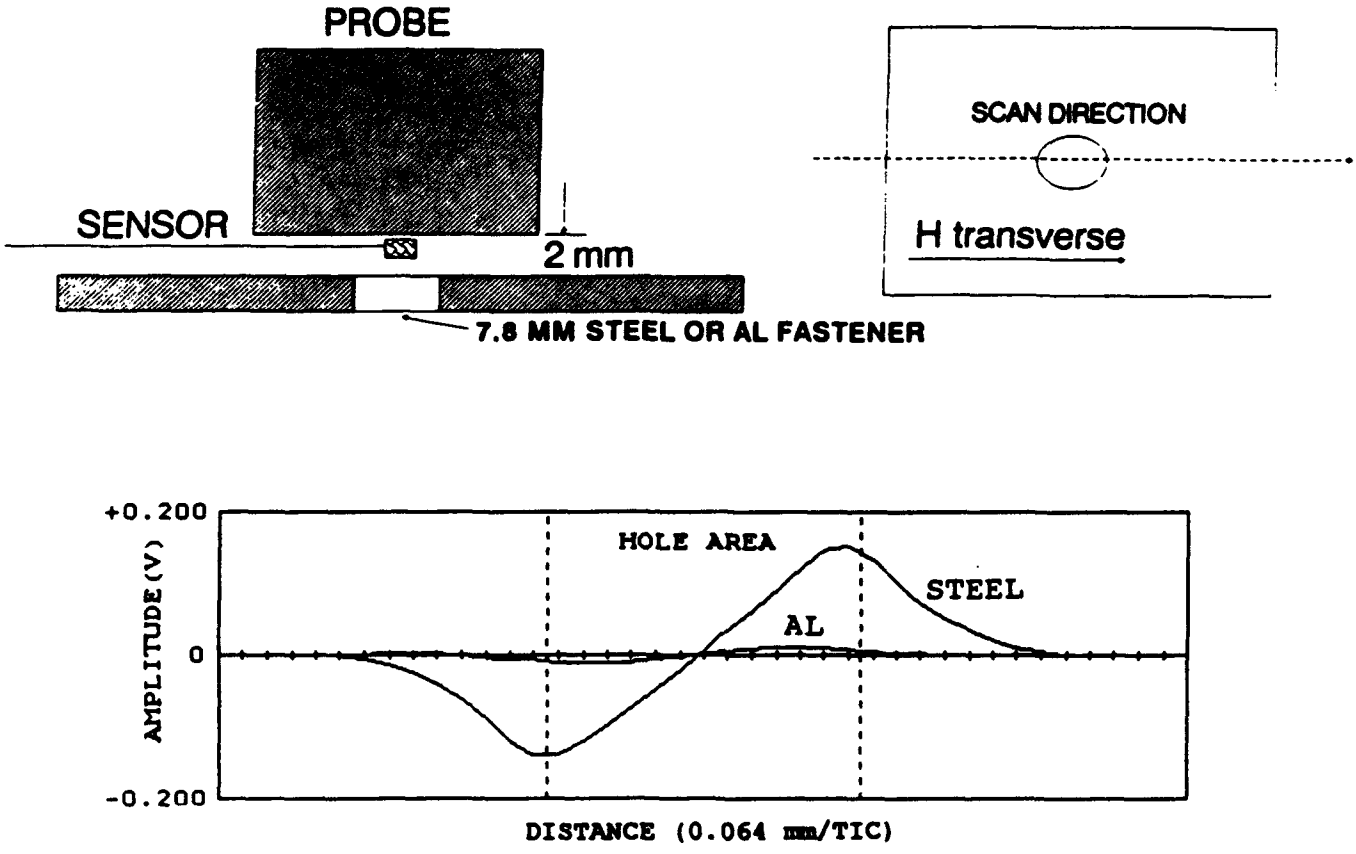


**FIGURE 10. TRANSVERSE MAGNETIC FIELD COMPONENT DUE TO A 7.8 mm STEEL FASTENER AND AN ALUMINUM FASTENER AT 600 Hz.**

Hz for an aluminum and a steel ferromagnetic fastener. The probe used in this test was a ferrite pot core with a solid center post that was the same diameter as the fastener hole. The probe induces a current in the head of the fastener. This current can reduce the sensitivity to CUFs by causing a response which cannot be fully accounted for in the compensation algorithms. Fastener head currents can be reduced by designing the probe core with a hole that is the size of the fastener head in the center, thereby minimizing the flux directed into the fastener head. This approach has been used in the past with good success.

The steel fastener also acts as an extension to the center post of the probe core. Figure 11 shows a scan of the transverse magnetic fields transmitted through a 6.3 mm (0.25-inch) thick aluminum specimen with a 7.8 mm (0.312-inch) steel fastener, an aluminum fastener, and through 6.3 mm of air. The sensor was scanned across the back side of the aluminum passing through the center line of the fastener. The magnitude of the through transmitted fields is greatly increased because of the steel fastener. The presence of the ferromagnetic steel fastener means the fields are excluded from the fastener hole and brought closer to the hole (less radial spread). At frequencies less than 1 kHz, the fields are of greater magnitude through the 6.3 mm (0.25-inch) aluminum skin with a steel fastener than through air at the same distance from the probe face. At frequencies greater than 1 kHz the shielding effect of the aluminum reduces the fields to less than the free air response, but the fields are always greater with a steel fastener than an aluminum or titanium fastener. As frequency is increased, the difference between the through transmitted fields for steel and nonferromagnetic fastener becomes less.

A result of the increased field strength because of the steel fastener is an increased sensitivity to features near the fastener hole. The sensitivity to off-center and CUFs is substantially greater at frequencies less than 1 kHz. Figure 12 shows a scan of the normal magnetic field component at 600 Hz at increasing off-center distances (0.2, 0.4, 0.6, 0.8 & 1.0 mm) or (0.008, 0.016, 0.024, 0.032, 0.04-inch). Compare this figure to Figure 8 which shows the same off-center conditions at 600 Hz, but without the steel fastener.

## Sense Coil Orientation and Placement

In an effort to improve the LFECA probe design it became apparent that an alternate sense coil placement would provide improved sensitivity. Several options are available for the arrangement of sense coils. Since sense coils could be placed on, against or away from the ferrite core the interaction between the core and sense coils needs to be considered in sense coil design. A series of experiments were performed to determine the effect of the ferrite core on the sense coil response for various placements and orientations within the core. A 3 mm diameter coil was used to simulate the current loop that would be caused by a CUF. The coil was scanned under the sense coil at 0, 2.5, 5.0 and 7.5 mm coil to coil distances to determine the relative spatial response of the sense coil. This is a crude approximation to the fields created by a CUF but does capture the essential character of the fields created by a CUF.

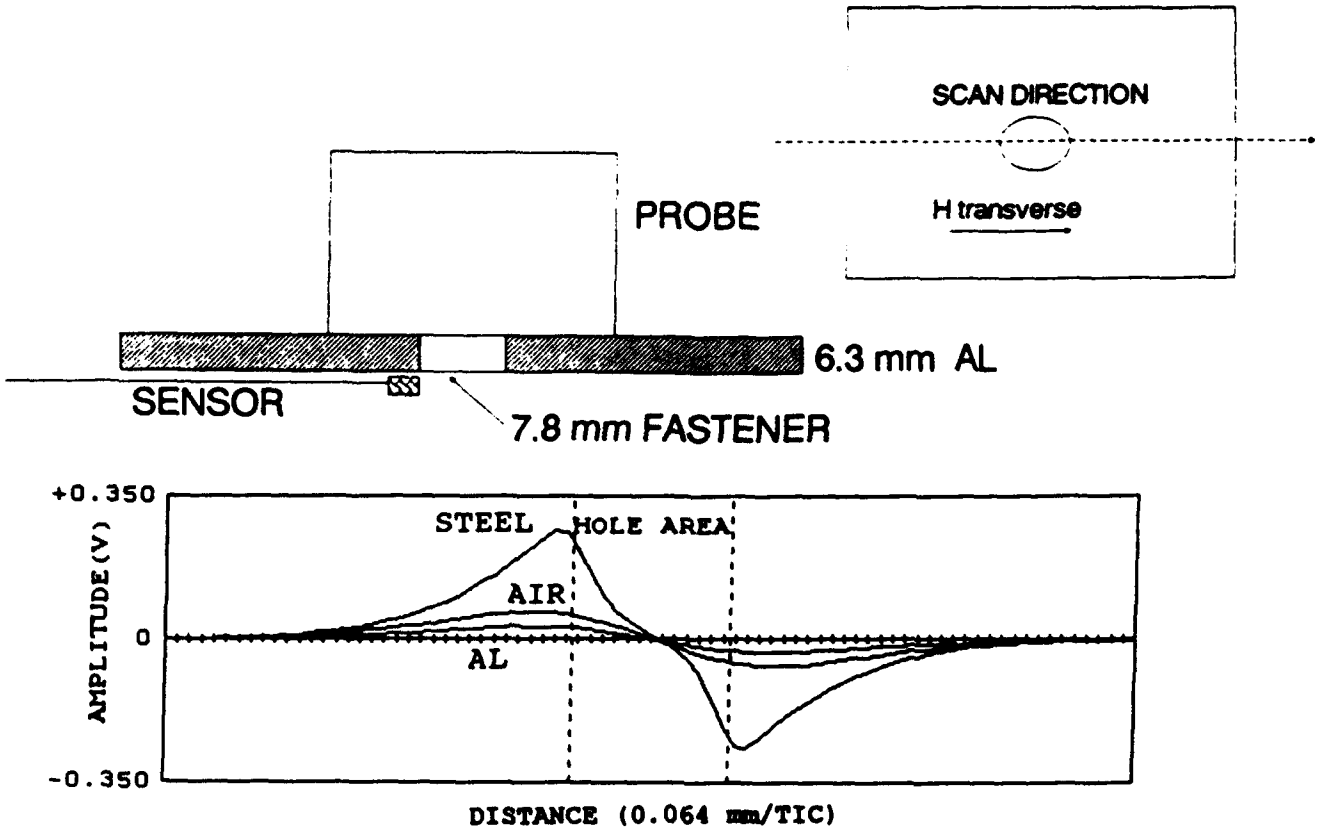


**FIGURE 11. TRANSVERSE MAGNETIC FIELDS TRANSMITTED through 6.3 mm OF ALUMINUM AT 200 Hz WITH A STEEL FASTENER, AN ALUMINUM FASTENER, AND THROUGH 6.3 mm OF AIR.**

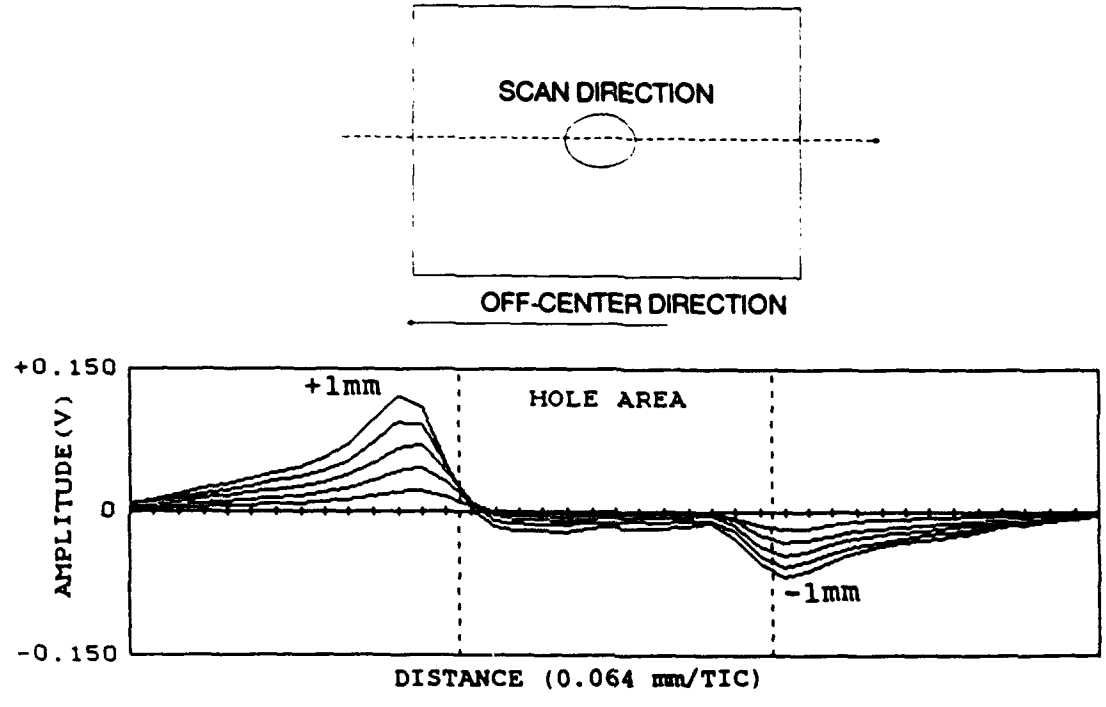


**FIGURE 12. NORMAL MAGNETIC FIELD COMPONENT AT THE PROBE FACE DUE TO OFF-CENTER (0.2, 0.4, 0.6, 0.8, AND 1.0 mm) WITH A STEEL FASTENER AT 600 Hz.**

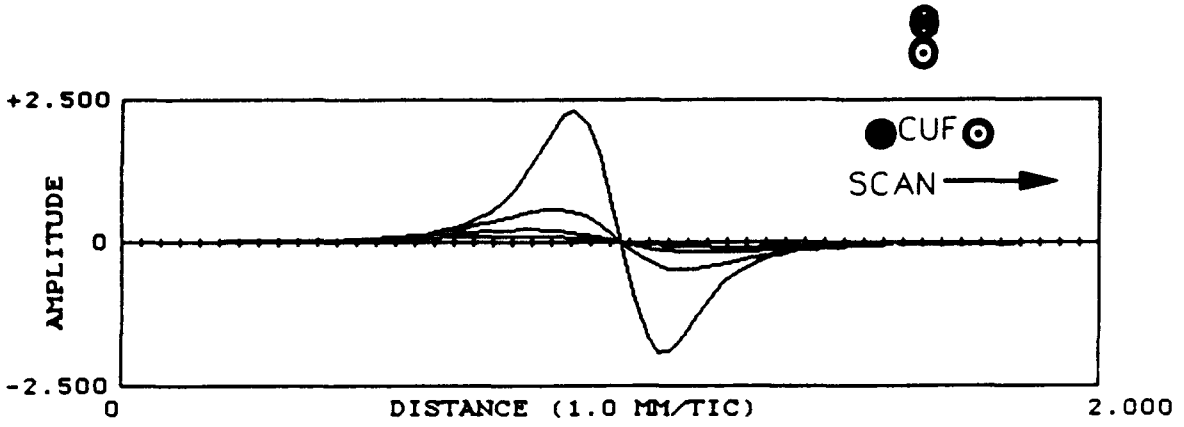


**FIGURE 13. SPATIAL RESPONSE OF A 2 mm DIAMETER SENSE COIL IN AIR AS A 3 mm DIAMETER COIL IS SCANNED BY AT DISTANCES OF 0, 2.5, 5.0 AND 7.5 mm. SENSE COIL IS ORIENTED TO DETECT THE TRANSVERSE MAGNETIC FIELD COMPONENT.**

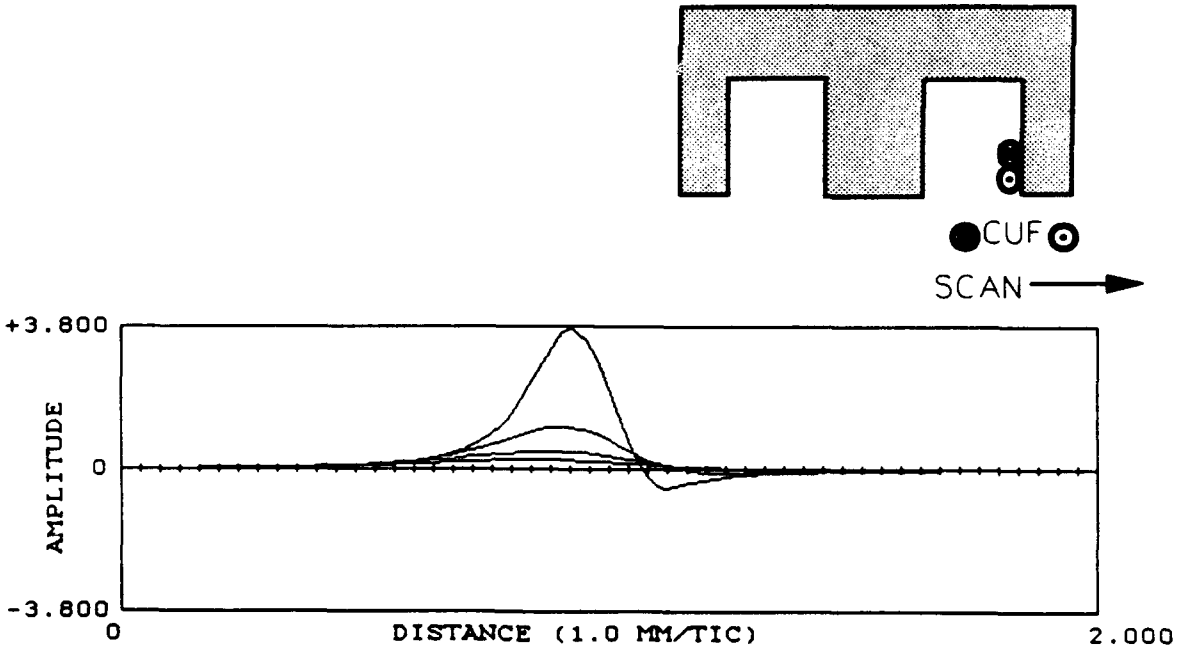


**FIGURE 14. SPATIAL RESPONSE OF SAME SET-UP USED IN FIGURE 13 WHEN THE SENSE COIL IS PLACED UP AGAINST THE FERRITE CORE.**

When a sense coil is placed next to the ferrite core you would expect the core to act as a shield which would modify the spatial sensitivity of the coil. Figure 13 shows the spatial response of a 2 mm diameter sense coil in air as the 3 mm diameter coil is scanned at coil-to-coil distances of 0, 2.5, 5.0, and 7.5 mm. The sense coil is oriented to detect the transverse magnetic field component generated by the simulated CUF. Figure 14 shows the spatial response when the same sense coil is placed up against the ferrite core with it's edge flush with the core face. Note that the ferrite core acts as a shield when it is between the sense coil and the source of the generated fields. The response magnitude is increased (10%) slightly and the sensitive region is more localized to directly under the sense coil. The increase in response magnitude is dependent on the width of the core with a wider core resulting in a greater response magnitude. The sensitivity with depth is also improved by 40% to 60%, e.g., sensitivity with depth drops at a slower rate. The shielding effect would be useful in reducing the sensitivity to adjacent structure and fastener head signals.

Figure 15 shows the spatial response if the sense coil is positioned centered between the core outer rim and center post. The coil is oriented to detect the transverse magnetic field component and is positioned flush with the core face. The core focuses the sense coil spatial response, reducing the sensitivity with depth and localizing the sensitivity to more directly under the sense coil. The response magnitude is also considerably reduced, a 70% reduction compared to the response when no core is present.

Whether the sense coil is against or away from the ferrite core the maximum sensitivity is achieved when the sense coil is as near to the face of the probe as possible. If the sense coil is recessed into the core the response magnitude will drop approximately 50% for every 1 mm the sense coil is recessed into the core. The spatial response is broadened with increasing recession into the core as would be expected even without the presence of the ferrite core.

A sense coil which is oriented to detect the normal magnetic field component is not as affected by it's placement within the core. Placing the sense coil up against the ferrite core does not significantly alter the spatial sensitivity of the coil either laterally or depth wise. Figure 16 shows the spatial responses of the 2 mm coil to the 3 mm CUF coil at distances of 2.5, 5.0, and 7.5 mm coil to coil distances. This sense coil was placed up against the side of the ferrite core flush with the core face. Recessing the sense coil into the core causes a rapid decrease in the response magnitude as well as a modest reduction in the response magnitude in the direction toward the ferrite core due to the core acting as a shield. For a sense coil oriented to detect the normal field component which is located flush with the core face, the core will have only a minimal effect.

Previous LFECA probe designs have had the sense coils placed on (rather than next to) the ferrite core. The sense coils are placed onto a post which is an integral part of the ferrite core. The sense coil having a ferrite core gives rise to a pronounced increase in the open circuit voltage induced by a magnetic field in the sense coil. A series of experiments were performed to evaluate the interaction of the sense coil and ferrite core when the sense coil is placed on the ferrite core.

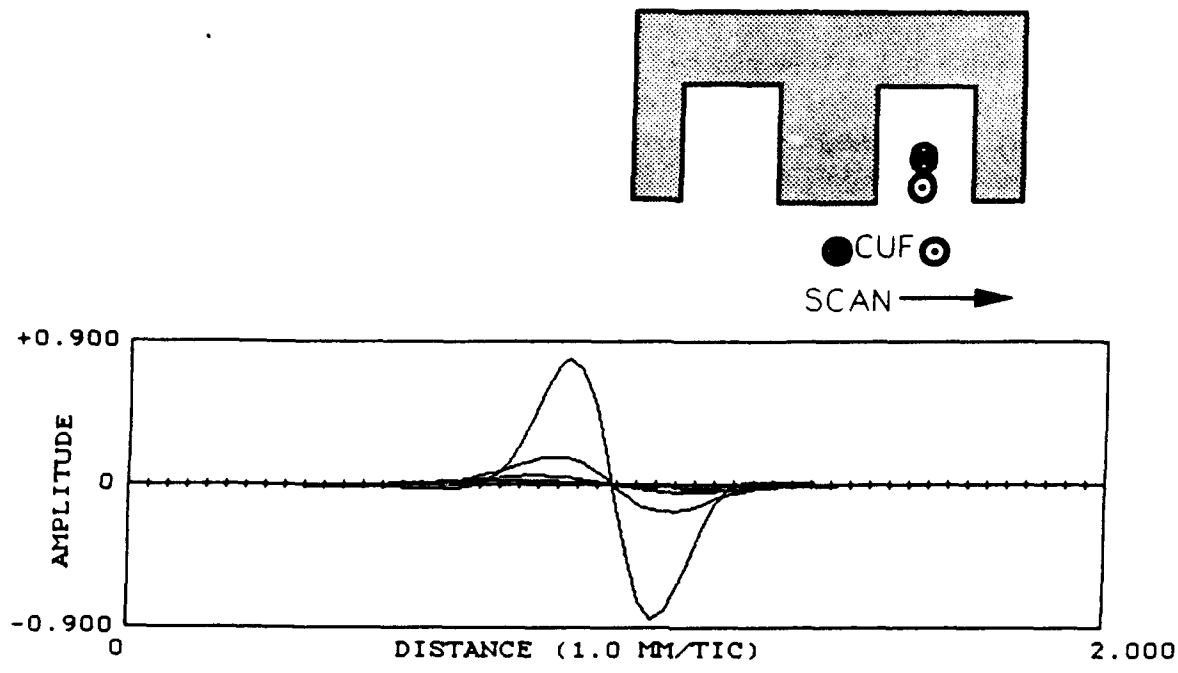


**FIGURE 15. SPATIAL RESPONSE OF SAME SET-UP USED IN FIGURE 13 WHEN THE SENSE COIL IS CENTERED BETWEEN THE CENTER POST AND OUTER RIM OF THE FERRITE CORE.**

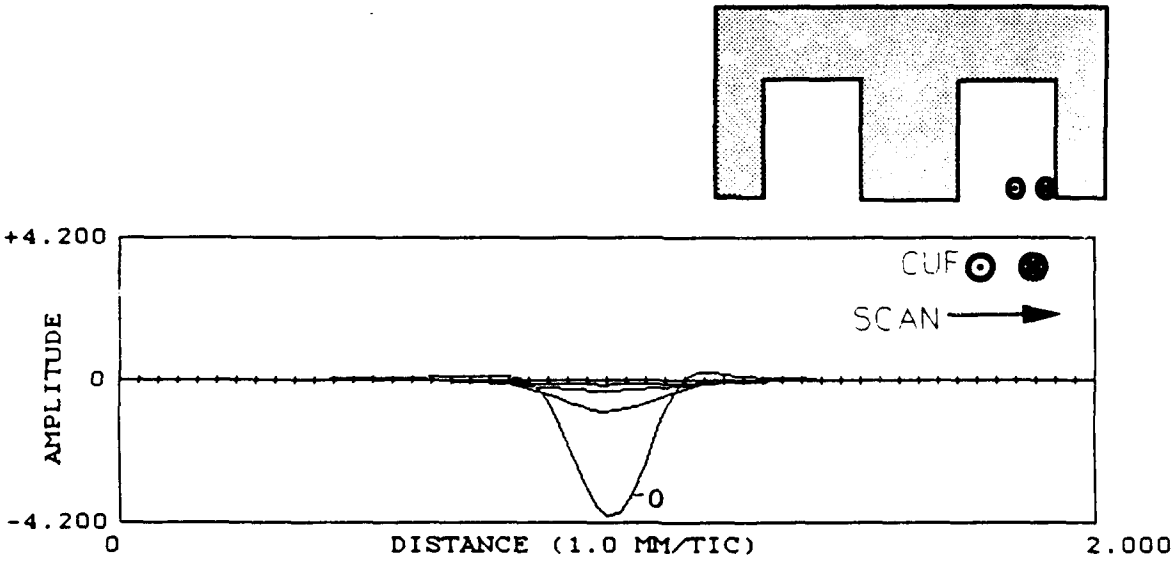


**FIGURE 16. SPATIAL RESPONSE OF THE SENSE COIL WHEN ORIENTED TO DETECT THE NORMAL COMPONENT OF THE MAGNETIC FIELD GENERATED BY THE 3 mm COIL SCANNED BY AT DISTANCES OF 0, 2.5, 5.0 AND 7.5 mm.**

To measure the effect of recessing the sense coil up a ferrite post, the 2 mm sense coil was placed on the end of a 2 mm diameter by 7 mm long ferrite rod and was scanned through the fields generated by the 3 mm CUF coil at coil to ferrite distances of 0, 2.5, 5.0, and 7.5 mm. Scans were performed with the sense coil flush with the end of the rod and at recessed distances of 1, 2.5, and 5.0 mm. This procedure was performed for both the normal and transverse orientations of the sense coil relative to the CUF coil.

For the normal oriented sense coil, the ferrite rod increased the response magnitude by 240% and was at a maximum in response when the sense coil was flush with the ferrite rod end. The response magnitude was unaffected by a 1 mm recess and drops by only 10% for every 1 mm of recession up the rod. This is approximately 20% of the rate at which the response magnitude decays with recession for a sense coil not on a ferrite core. As the sense coil is recessed up the ferrite rod the spatial response broadens and the depth response improves. Figures 17 and 18 show the spatial responses at 0 and 5.0 mm recession. Note that at a distance of 7.5 mm from the end of the rod, the 5 mm recessed coil has 1.7 times the response magnitude as the 0 mm recessed coil. Recessing the sense coil results in an improved depth sensitivity at the cost of spatial resolution. The effect is comparable to making the sense coil larger in diameter with fewer windings.

## Multiple Sense Coil Arrays and Sense Coil Placement

In order to discriminate between different effects such as CUFs, edges, and off-center, multiple parameters need to be measured. One way of accomplishing this is to use multiple concentric arrays to measure the radial distribution of the magnetic fields induced by the probe. To simulate multiple concentric arrays and to also evaluate the effect of sense coil placement, a core with five sense coils was constructed as shown in Figure 19. The coils were all oriented to detect the magnetic field normal to the probe face. Of the five coils, four were placed at increasing radial distance from the center of the probe and one coil (coil 3) was a larger area coil which was effectively the equal of the integral of the two innermost coils (coils 1 & 2). Coils 1, 2 and 3 were between the center post and outer rim of the probe core. Coil 4 was located on the outer rim of the ferrite core and is representative of the previous LFECA probe designs and provided a means in which to compare these results to prior LFECA probe results. Coil 5 was located outside the outer rim of the core.

A series of evaluations were performed to compare the response characteristics of the coils to CUFs, edges and etc. The following is a summary of the observations derived from these tests:

### Second Layer CUF Response

For thinner metallic skins, the sense coil located closest to the probe center or fastener hole wall (coil 1) has an increased sensitivity and sharper spatial response to a small CUF. The sense coil response to a small CUF decreases with radial distance from the probe center, e.g. coil 1 > coil 2> coil 4 > coil 5. There is also a slight broadening of the spatial response and a shift in phase response with increasing radial distance. All the above observations are consistent with the CUF perturbed magnetic fields being restricted to

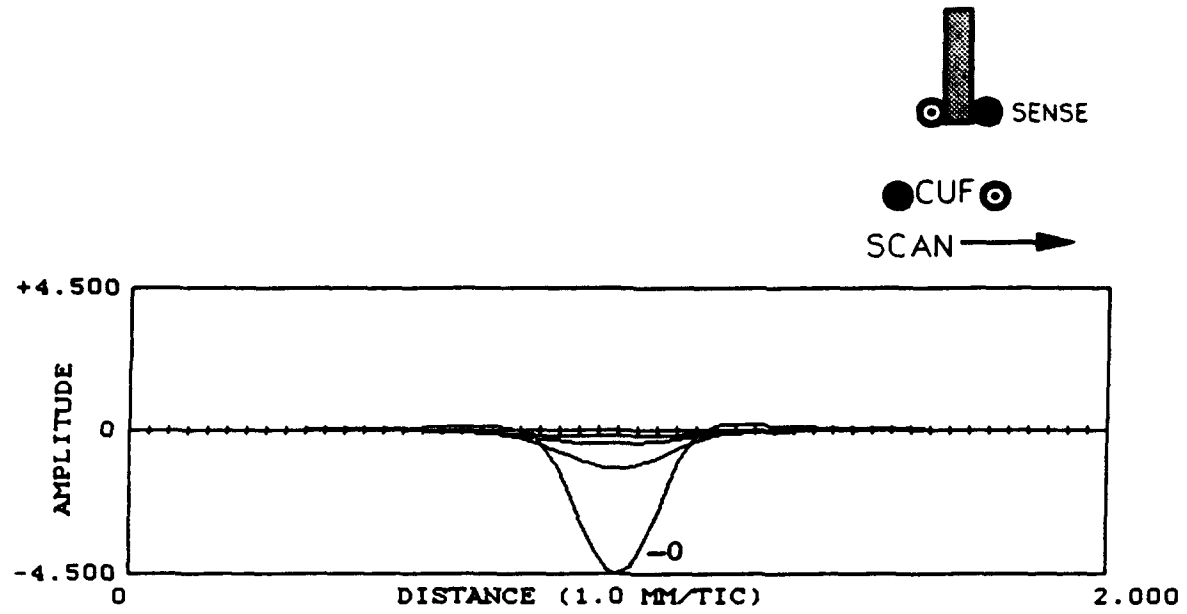


**FIGURE 17. SPATIAL RESPONSE OF SENSE COIL MOUNTED FLUSH ON END OF FERRITE ROD AT DISTANCES OF 0, 2.5, 5.0 AND 7.5 mm.**

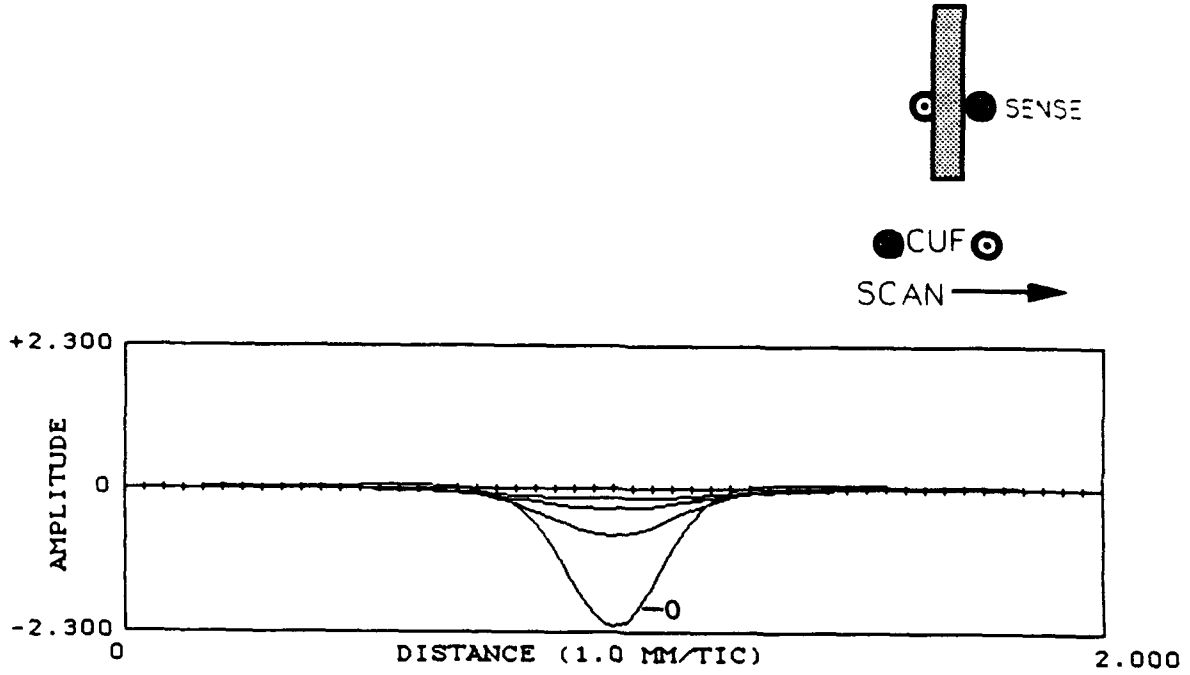


**FIGURE 18. SPATIAL RESPONSE OF SENSE COIL RECESSED 5.0 mm FROM END OF FERRITE ROD AT DISTANCES OF 0, 2.5, 5.0 AND 7.5 mm DISTANCES.**

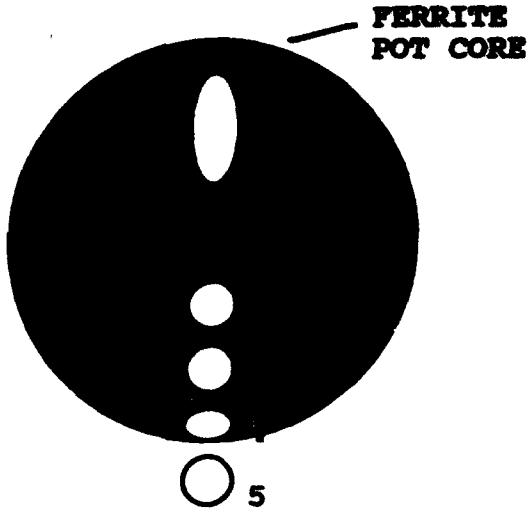


**FIGURE 19. VIEW OF PROBE FACE SHOWING SENSE COIL PLACEMENT FOR SIMULATING MULTI-ARRAYS AND DIFFERING SENSE COIL PLACEMENT. FIVE SENSE COILS ARE SHOWN, FOUR AT INCREASING RADIAL DISTANCE FROM THE PROBE CENTER AND ONE LARGER SENSE COIL.**

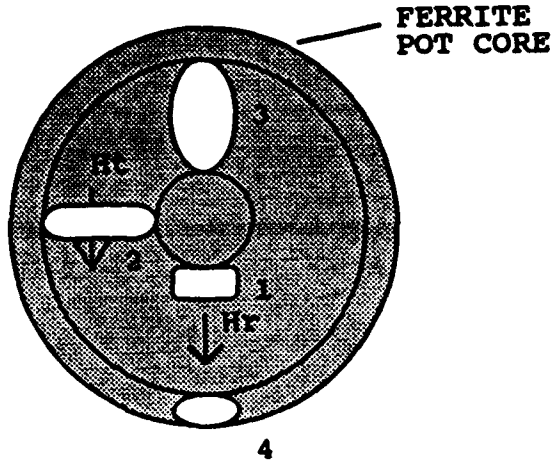


**FIGURE 20. VIEW OF PROBE FACE SHOWING LOCATION OF THE DIFFERENT ORIENTATION SENSE COILS. COILS ORIENTED TO DETECT THE RADIAL (COIL #1), TANGENTIAL (COIL #2), AND NORMAL (COILS #3 AND #4) MAGNETIC FIELD COMPONENTS ARE SHOWN.**

more directly over the CUF (for thin skins 3 mm or less). An absolute gain in sensitivity to small CUFs of over 200% can be achieved for thinner skins by moving the sense coils inward from the outer rim ( coil 1 vs. coil 3).

For thicker skins, the difference between the response magnitudes of sense coils 1 to 4 due to a CUF are much smaller. An increase in skin thickness results in a significant spreading of the CUF perturbed magnetic fields and therefore less variation in response with changing radial distance. The general conclusion to be drawn from these results is that to maximize CUF sensitivity when inspecting through thicker skins there is little benefit to using multiple concentric arrays located within the core (such as the coils 1,2, and 4). The additional information (radial dependence of response) gained is not very helpful for improving CUF sensitivity. Although it could be useful for determining CUF size since there is a response difference indicative of CUF length. An array made from coil 3 or a larger coil which would extend under the ferrite rim (essentially coil 3 plus coil 4) offers the greatest sensitivity to CUFs.

There is a practical limitation to the use of multiple arrays due to the requirement for the sense coil output to be above the electrical noise level. Since the coil output is proportional to coil area and number of turns, there is a minimum size for the coil. For an air coil the depth of a sense coil is limited to approximately 5 mm, any additional depth is not effective. A requirement for a minimum size will eliminate the possibility for multiple arrays located within the core to only the larger cores sizes. For the 1 micro-volt noise level present in the LFECA system electronics this limits the coil size to about a 2.5 mm diameter coil to detect a 1.25 mm second layer CUF through a 6.4 mm skin given the current probe drive current. A sense coil on the ferrite core has a higher output (approximately three times) due to the effective permeability of the ferrite. An increase in sense coil output can also be achieved by increasing the drive current but requires that the probe be designed to dissipate the heat developed by the higher drive currents.

**First and Second Layer Edge Response**

The response magnitude of a sense coil to an adjacent edge is proportional to the edge-to-coil distance. For an edge which lies outside the probe diameter (which would be the typical case) the sense coil response magnitude is greatest for coil 5 which is located outside the probe and is smallest for coil #1 which is closest to the probe center. Coils 1, 2 and 3 have a 300% to 400% smaller second layer edge response than coil 4 for a typical second layer edge distance. This magnitude of decrease in edge response for coils moved closer to the probe center occurs for thinner (3 mm) and thicker skins (6.4 mm). Coils 1, 2, and 3 have a 1000% smaller response for a typical first layer edge compared to coil 4. Each coil also has a phase response which is dependent on the edge to coil distance. A significant decrease in edge response can be achieved by moving the sense coil in a radial direction inward. A compromise exists between increasing the sense coil size for better second layer CUF detection through thick skins and reducing the radial size of the sense coil to minimize edge sensitivity. The factors in determining the best compromise are the skin thickness, minimum detectable CUF, and edge distance. These factors will not be constant from application to application making a compromise based on the average values for these factors the optimum approach.

A multiple array approach using coil 5 (coil outside of core) to form an additional array has some merit for edge compensation. Coil 5 has a high sensitivity to adjacent edges with a sharp spatial response and phase response dependent on edge distance. This outer array also has only a small sensitivity to CUFs and a very broad spatial response to a CUF. A probe with an array inside (coil 3) and an array outside (coil 5) the probe core would provide two responses with very different sensitivity to edge and CUF. The two responses do not provide separate measurements of each response or orthogonal data sets. They can be made to be partially orthogonal by recognizing the spatial and phase response differences. Using an outer array is a design alternative (or addition) to using multiple drive coils with a drive coil around the outside of the core.

### Off-Center Response

The off-center response for all five coils was essentially a single period of a sine wave (predominately fundamental frequency). The sensitivity to off-center is greatly effected by moving the sense coil in towards the center of the probe. Coil 1 is about 4 times more sensitive than coil 4 and is about twice as sensitive as coil 2. Coil 3 is about three times as sensitive as coil 4. Coil 3's response characteristics closely approximate the average of coils 1 and 2. A higher sensitivity to off-center is also indicative of a higher sensitivity to first layer CUFs. The phase of the off-center response can be made to be very close to orthogonal to a second layer CUF by selecting the appropriate drive frequency. For example, at 400 Hz the off-center response and the second layer CUF response through 6.4 mm aluminum are very close to being orthogonal in phase response. An increase in off-center sensitivity is not a desirable effect. However, an off-center response is the most linear, repeatable and least difficult effect to compensate for using a combination of multifrequency and phase discrimination methods.

## Multiple Sense Coil Arrays and Sense Coil Orientation

Three basic sense coil orientations were investigated each oriented to detect a polar component of the magnetic field. A probe with four sense coils was constructed, one for each of the basic orientations and one coil placed on the outer rim of the ferrite core, Figure 20. Coil 1 was oriented to detect the radial magnetic field component, coil 2 was oriented to detect the tangential magnetic field component and coil 3 detected the field normal to the probe face. Sense coil 4 was located on the ferrite core and is representative of the previous LFECA probe designs and provided a means of comparing to prior LFECA probe results. A series of evaluations were performed to compare the sensitivity and response characteristics to CUFs, edges, off-center and etc. A summary of the results of these evaluations follows:

A sense coil oriented normal to the probe face will have the greatest output due to a CUF. Using a coil oriented in another orthogonal direction will result in a 200% to 400% lower output. However, the idea was that a differently oriented coil could have a lower sensitivity to adjacent edges. With the result that the ratio of edge to CUF response would be much smaller making compensation for edges an easier task.

For Coil 1 (radial magnetic field component), the CUF sensitivity was reduced for CUFs smaller than the coil size, especially for thinner skins and at higher frequencies. The ratio of edge/CUF and off-center/CUF were not improved compared to these same ratios for coil 3 (normal magnetic field component). Also, placing this coil near the probe center post to maximize CUF sensitivity places the coil in the way of a protruding fastener unless the coil is recessed which will reduce its sensitivity. Moving the coil in a radial direction outward away from the fastener head also reduces sensitivity to small CUFs. From a practical stand point, it is also rather difficult to construct a probe with a high enough CUF sensitivity using small enough radially oriented sense coils with the present LFECA electronics.

For Coil 2 (tangential magnetic field component) the ratios of (first layer edge)/CUF, (second layer edge)/CUF, and off-center/CUF response were not improved over these same ratios for Coil 3 (normal magnetic field component). There wasn't a significant decrease in the sensitivity to edges and there was a slight increase in off-center sensitivity. The spatial response to CUFs and edges differed from those due to off-center. Figure 21 shows the response shape typical of an edge or CUF and the response shape typical of an off-centered condition. Off-center results in a response which is nearly a single period of a sine wave. A CUF or edge response has a much higher amount of second and third harmonic content due to the response being at a null directly over the CUF or adjacent to the edge. This feature could be used to help remove an off-center response. A probe with a combination of normal and tangential oriented sense coils may be an attractive design alternative in some cases.

### 2.1.2 Drive Coil And Core Shape Optimization

The basic goal in optimizing the drive coil and core shape is to maximize the eddy current distribution at the fastener hole wall. Ideally this would be achieved without creating eddy currents which could be perturbed by adjacent structure. Since this is apparently not possible the design criteria is one of compromise. A series of analytical and experimental evaluations was performed to determine the reasonable design alternatives. Experiments were performed to evaluate the effect of drive coil, sense coil and core design on CUF sensitivity and compensation algorithm development. The following is a summary of the results of these experiments, along with a discussion of their effect on LFECA probe design and algorithm development.

#### Core Shape Optimization - Pot Core Shape

The previous LFECA probe designs used a ferrite pot core as its rudimentary design element. The core dimensions can be optimized for the particular application. The basic dimensions are the center post size and shape (solid or hollow), outer rim diameter and width, and depth of the probe. A series of experiments were performed in which a variety of cores having a range of dimensions were studied to determine their efficiency and field profiles. These data were compared with analytic calculations previously performed for differing core shapes. The following is a narrative of conclusions which have been derived from this analysis.

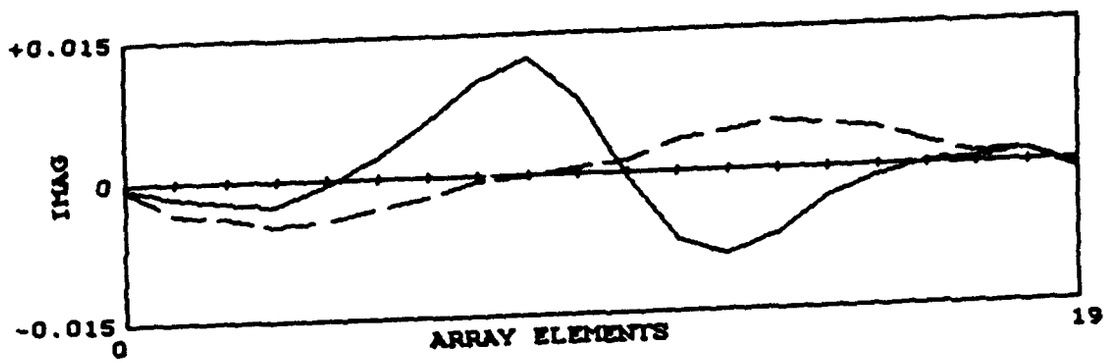


**FIGURE 21. TYPICAL OFF-CENTER RESPONSE (DASHED LINE) AND CUF RESPONSE (SOLID LINE) FOR TANGENTIAL MAGNETIC FIELD COMPONENT, SENSE COIL #2. A SINGLE ROTATION OF 360 DEGREES WAS DIGITIZED EVERY 18 DEGREES FOR A TOTAL OF 20 SEGMENTS.**

For the case of a nonferromagnetic fastener, the center post diameter is not a critical dimension but should be approximately the size of the fastener hole. Increasing the center post diameter will move the eddy current distribution in a radial direction away from the fastener hole. This will result in reducing the sensitivity to first layer CUFs and to a lesser degree will reduce the sensitivity to second layer CUFs.

For the case of a ferromagnetic fastener (steel), the choice of a center post becomes a more critical factor. A center post which is the diameter of the hole will allow a large amount of eddy currents to be induced in the fastener head. The steel fastener will also effectively act as an extension to the ferrite center post drawing the fields into the metallic substructure. The result will be a probe which is very sensitive to the fastener head and also has excellent sensitivity to CUFs.

To compensate for the large response attributable to a fastener head being oval, crooked or marked, a multifrequency compensation scheme can be used. In the past this approach has not always worked perfectly due to the large difference in magnitudes between a typical fastener error response (20 mV) and a second layer CUF response (2 mV).

A solution used in the past was to enlarge the center post diameter and place a hole down the center of the center post which was the diameter of the fastener head. This eliminated any problem with sensitivity to the fastener head but also reduced the sensitivity of the probe since it was not coupled as well to the fastener. Sensitivity to near surface CUFs is reduced more than second layer CUF sensitivity since there is little current induced directly under the fastener head. Further down the fastener shank the induced current level is not as effected since the current spreads out with increasing depth.

A key to a successful design is to optimize the center post shape and size so that it will effectively couple the probe to the fastener but generate minimal fields in the surface of the fastener head. This requires some compromise between sensitivity to the fastener head and CUF sensitivity. The best compromise appears to be making the center post a slightly larger diameter than the fastener head (typically 1 mm) and the hole down the center of the center post which is slightly smaller than the fastener head. The portion of the center post which is smaller than the fastener head will need to be slightly recessed (typically .25 mm) to allow for a slightly protruding fastener. This will result in a fair amount of coupling to the fastener without becoming sensitive to the markings on the fastener head which can be difficult to remove using compensation methods. Compensation for fastener related error signals will be required, however, the size and spatial shape of the response will be within limits which will make it a reasonable exercise.

The core outer rim can be thought of as performing two functions, it constrains the magnetic fields within its walls thereby reducing the probes footprint and it reduces the reluctance of the magnetic field path within the probe thereby increasing the efficiency of the probe. The choice for outer rim diameter is restricted to a large degree by practical limitations. The probe diameter needs to be such that it can sit flat on the surface and also

have a reasonably limited sensitivity to adjacent structure. The aircraft design guideline generally followed for the distance from the fastener hole centerline to an adjacent structural edge is 2D + 1.5 mm ( where D is the hole diameter). This forces an upper limit for the outer rim diameter of approximately 4D (where D is the hole diameter). Since the hole diameter and skin thickness generally increase together this limitation will generally allow an adequate diameter drive coil for the required penetration depth.

Figure 22 shows a sketch of the drive coil and ferrite core used for the measurements presented in Figures 23 and 24. Magnetic field measurements were taken by scanning a single line perpendicular to and through the coil centerline on the other side of an aluminum plate. The transverse magnetic field direction and the scan direction relative to the coil are indicated in the figure.

Figure 23 shows the magnitude of the transverse magnetic field generated through 5.1 mm of aluminum at 400 Hz. Two curves are shown: one for a drive coil with a ferrite pot core and the same drive coil without a ferrite core. The eddy current distribution induced in the aluminum will be the same shape as these curves. The outer rim of the ferrite core focuses the current distribution thereby reducing the sensitivity to adjacent structure. However, note that the peak in the fields occurs approximately 6.4 mm from the centerline of the coil. This would mean that the peak current would not occur at the fastener hole wall unless the hole were a 6.4 mm radius. The best sensitivity to cracks radiating from the fastener hole wall is achieved when the current is localized (and maximized) at the fastener hole wall. When using a pot core shaped design, localizing the eddy currents usually requires reducing the core size which also reduces depth penetration. Figure 24 shows an example of the effect of drive frequency on the field distribution. This figure shows the field generated through 3.8 mm of aluminum at 400 Hz and at 10 kHz. The aluminum acts as an effective shield at 10 kHz localizing the fields to more or less directly under the drive coil (currents near the centerline and in a radial direction outward are reduced) as well as reducing the field magnitude. The 400 Hz curve is very similar to that which is obtained without the aluminum present ( free space response).

Figures 25 and 26 show examples of the magnetic fields produced by ferrite pot cores with a 31 mm outer diameter and a 18 mm outer diameter using the same 16 mm outer diameter drive coil. These two cores would be appropriate for inspecting around a 7.9 mm fastener which could have an adjacent edge at 16 to 18 mm from the hole centerline. The smaller diameter core produces field magnitudes which are greater than 4 times that of the larger core. The fields drop off more rapidly with depth (9% Vs 12% of surface magnitude at 7.5 mm ) and are also constrained by the smaller core to more directly under the core. The smaller core would be appropriate for inspecting under 6 mm skins and is considerably smaller diameter than the practical limit for core diameter determined by adjacent structure. The selection of core diameter is a compromise between constraining the fields and depth penetration. The guidelines for this compromise have been established in this and previous studies.

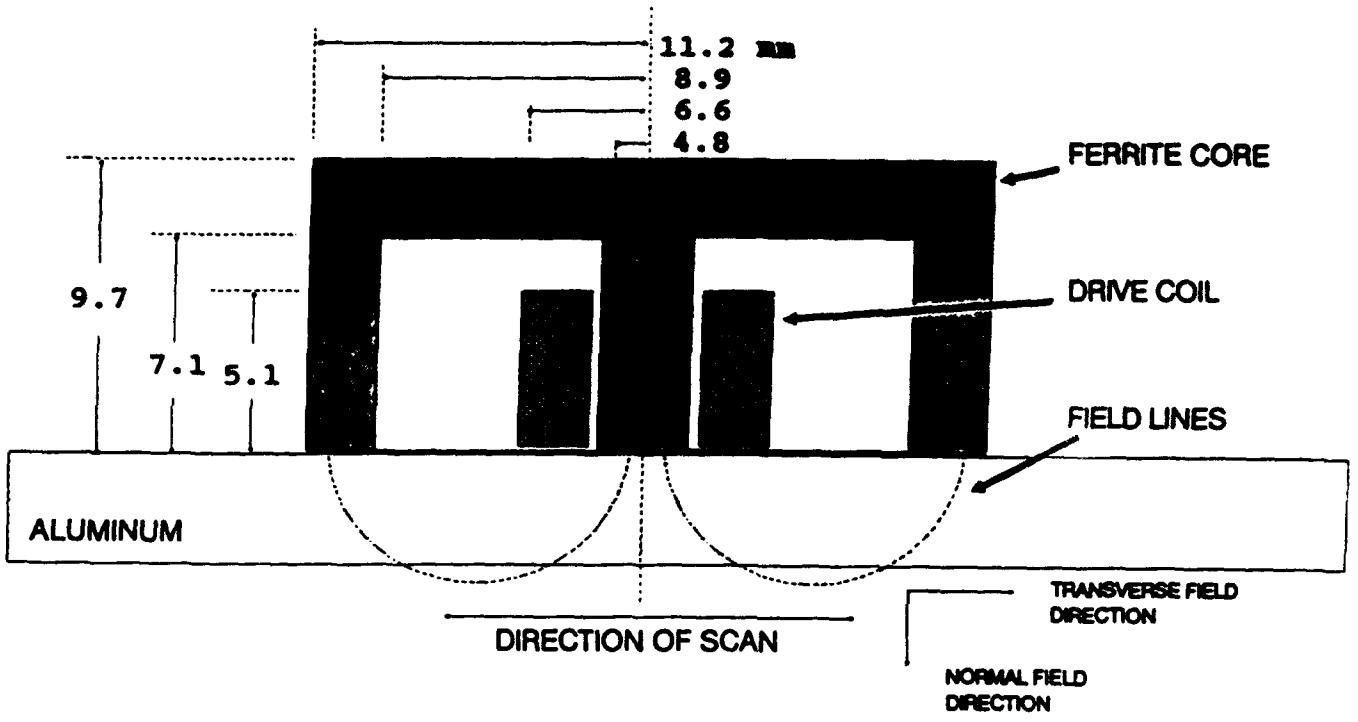


**FIGURE 22. FERRITE CORE AND DRIVE COIL CONFIGURATION FOR FIELD MEASUREMENTS PRESENTED IN FIGURES 23 AND 24.**

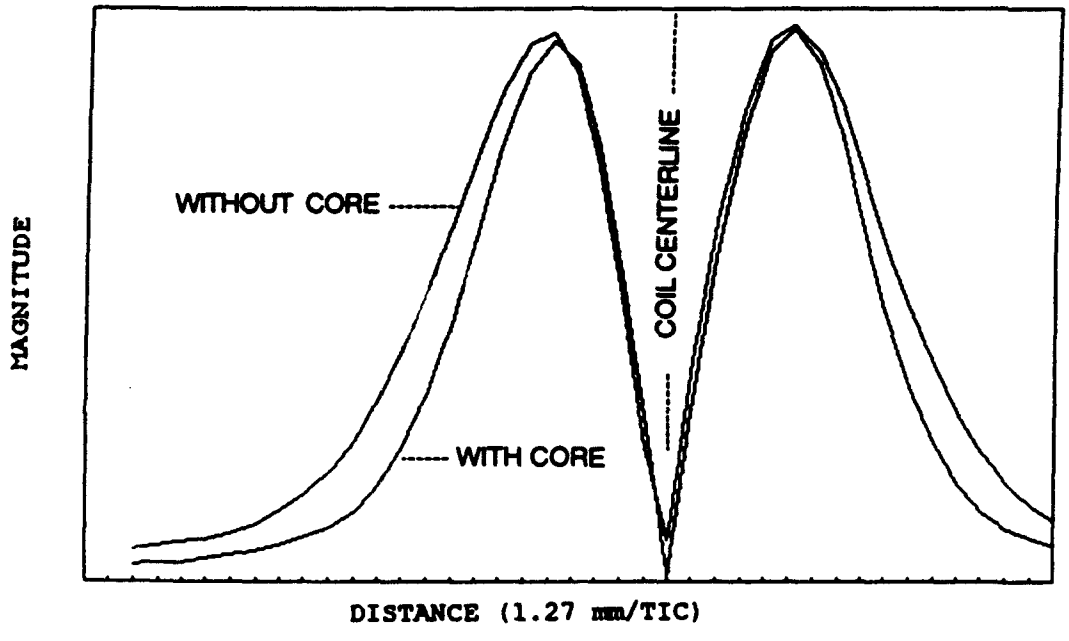


**FIGURE 23. MAGNETIC FIELD PROFILE THROUGH 5.1 mm OF ALUMINUM FOR A DRIVE COIL WITH AND WITHOUT A FERRITE CORE AT 400 Hz.**

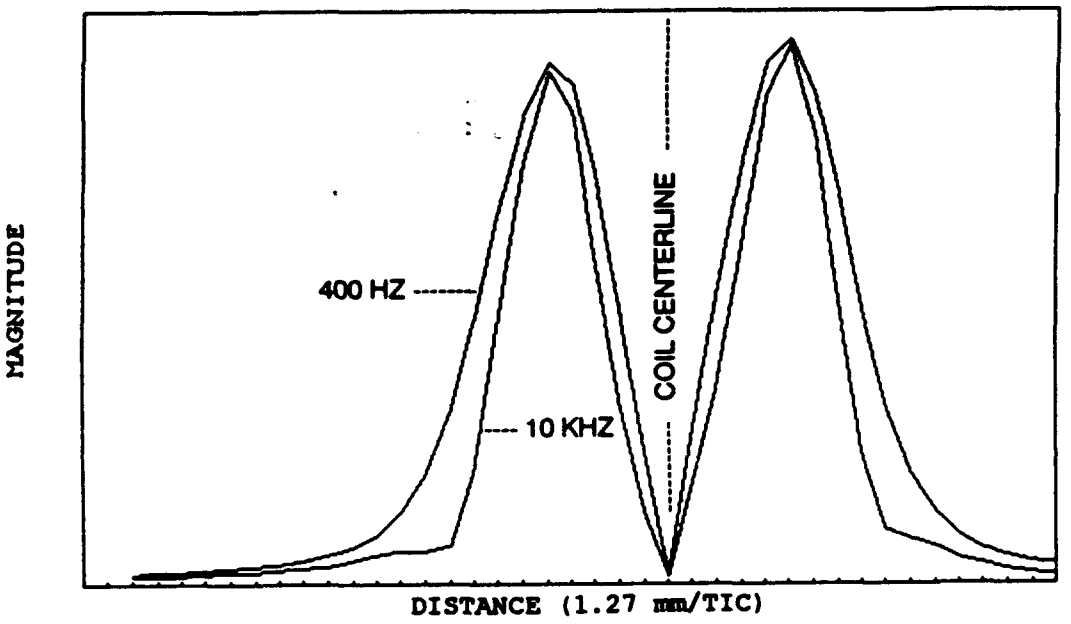


**FIGURE 24. MAGNETIC FIELD PROFILES THROUGH 3.8 mm OF ALUMINUM AT 400 Hz AND AT 10 kHz DRIVE FREQUENCIES.**

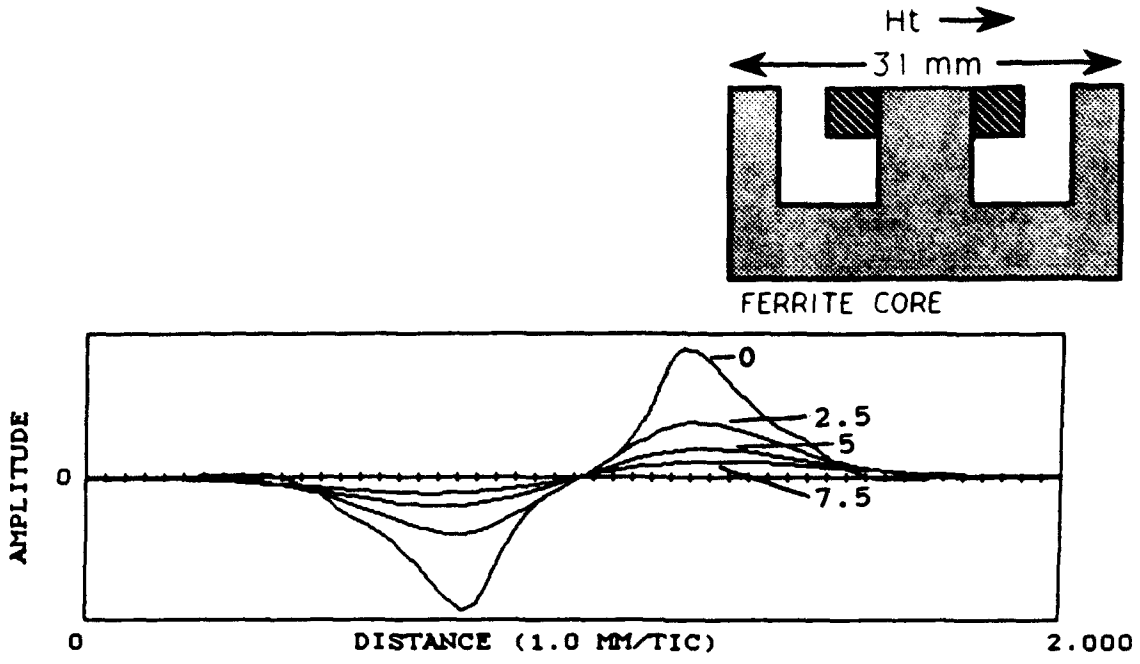


**FIGURE 25. TRANSVERSE MAGNETIC FIELDS GENERATED IN AIR BY A 16 mm OUTER DIAMETER DRIVE COIL ON A FERRITE POT CORE WITH A 31 mm OUTER DIAMETER AT DISTANCES OF 0, 2.5, 5.0, AND 7.5 mm FROM THE CORE'S FACE.**

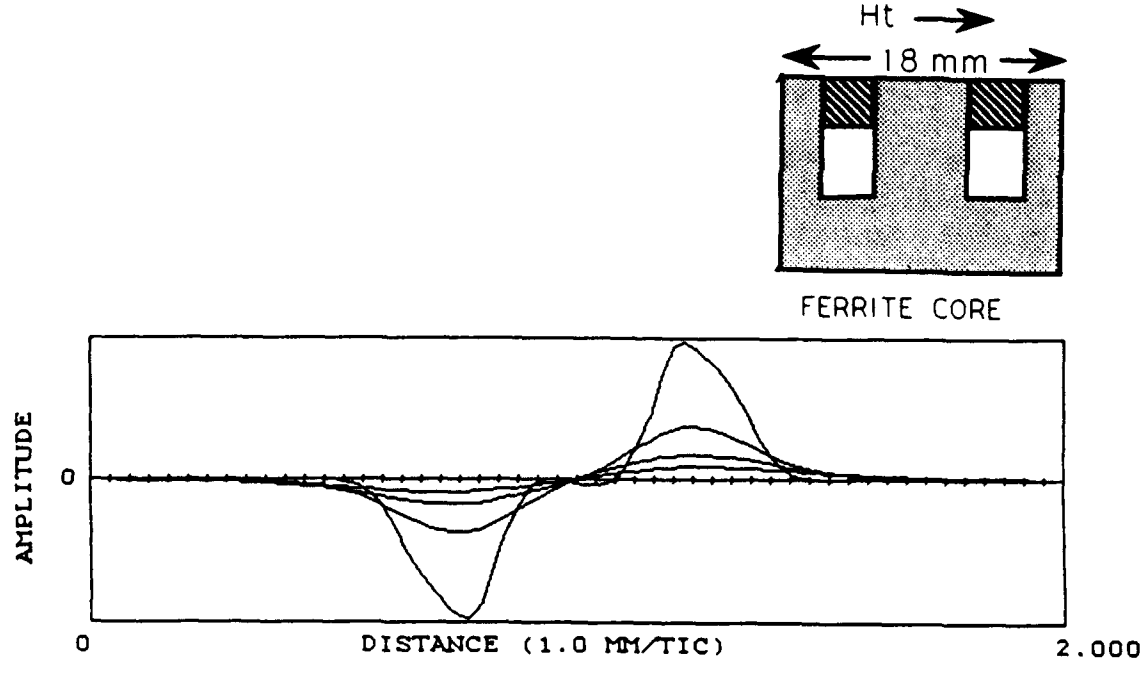


**FIGURE 26. SAME SET-UP AS FIGURE 25 BUT WITH A SMALLER DIAMETER FERRITE CORE OF 18 mm.**

Within the practical limits for probe height, the core depth is chosen based on the impedance required by the driving circuitry. A depth capable of allowing the required number of windings of the appropriate gauge wire (which is dependent on power dissipation limitation) is chosen based on simple calculations.

## Alternate Core Shapes

For the case of the nonferromagnetic fastener an alternate core shape may be attractive. When a fastener made from a low electrical conductivity material such as a titanium or stainless steel is to be inspected the fastener hole could be considered a low conductivity hole into the underlying structure. A magnetic field could penetrate down through this hole with a much lower attenuation due to skin effects. This would allow the use of much higher inspection frequencies with a resulting increase in eddy currents in the fastener wall and a decrease in eddy currents generated away from the hole.

Figure 27 shows a sketch of an elongated c-core probe which when placed over a fastener would generate a magnetic field that would penetrate down the hole. The c-core shape also has a better penetration capability than a pot core shape. Figure 28 shows the field detected at distances of 0, 2.5, 5.0, and 7.5 mm from the c-core face. If you compare this figure to Figure 26 you will note the better depth dependence, at 7.5 mm the field magnitude is reduced to 33% versus 10% of its magnitude at the surface (0 mm). Figure 29 shows the fields generated on the opposite side of a 6.3 mm thick aluminum skin through a 7.9 mm hole when the elongated c-core is used at 10 kHz. The radial spread of the fields is reduced by increasing the inspection frequency and still penetrates through the hole. Since the current generated by this shape of core will not evenly encircle the hole as does a pot core shape, either the core will need to be rotated or a multiple drive configuration will be required to achieve equal sensitivity around the hole. Several possible design configurations have been devised which would solve this problem. Figure 30 shows the fields transmitted through a 6.3 mm aluminum skin with a 2.5 mm slot or a 5.0 mm slot radiating from a 7.9 mm hole at a 10 kHz inspection frequency. Notice that the fields over the hole are disturbed by the slot, indicating that these fields will be radiated up the hole (through a low attenuation path) where they could be detected using a sense coil array located in close proximity to the hole. The sense coil array could be made to encircle the hole, could be in a linear arrangement, or could be made up of single or dual elements which rotate with the core.

## Drive Coil Optimization

The effect of drive coil shape and placement within the probe core was investigated to determine the optimum drive coil shape for field generation and to determine the viability of a multiple drive coil design approach.

The interaction of ferrite core and drive coil windings was demonstrated by investigating a number of cases representative of possible LFECA probe designs. An example which will be representative of these experiments is one in which the fields generated by two extremes in drive coil shape in a ferrite pot core were studied. One coil

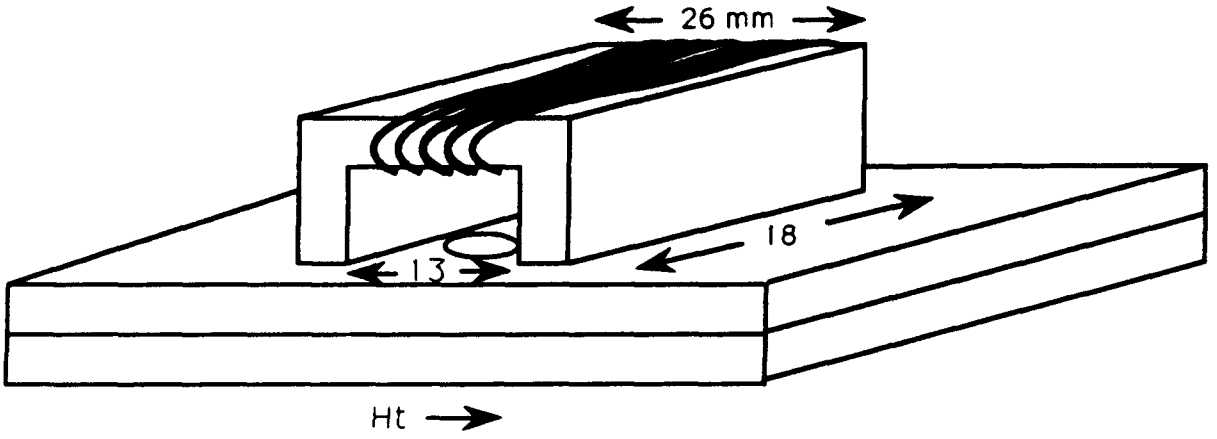


**FIGURE 27. ELONGATED C-CORE PROBE OVER A FASTENER HOLE.**

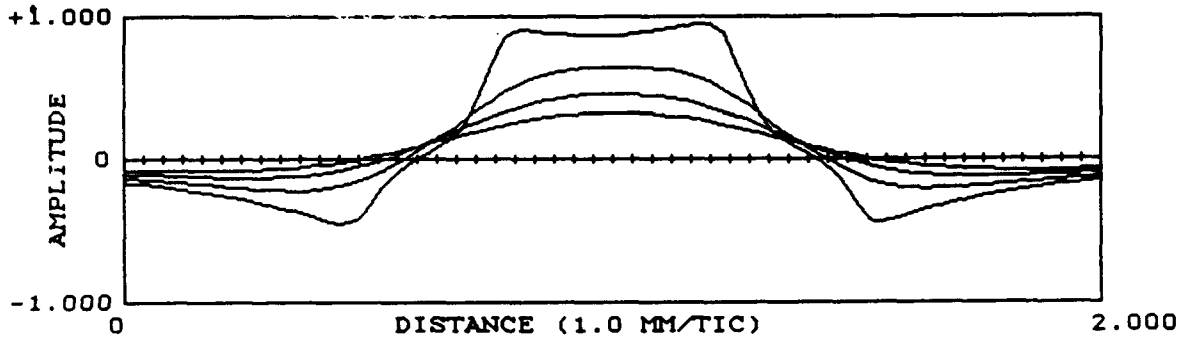


**FIGURE 28. TRANSVERSE MAGNETIC FIELD GENERATED IN AIR BY ELONGATED C-CORE PROBE AT DISTANCES OF 0, 2.5, 5.0 AND 7.5 mm FROM THE CORE FACE.**

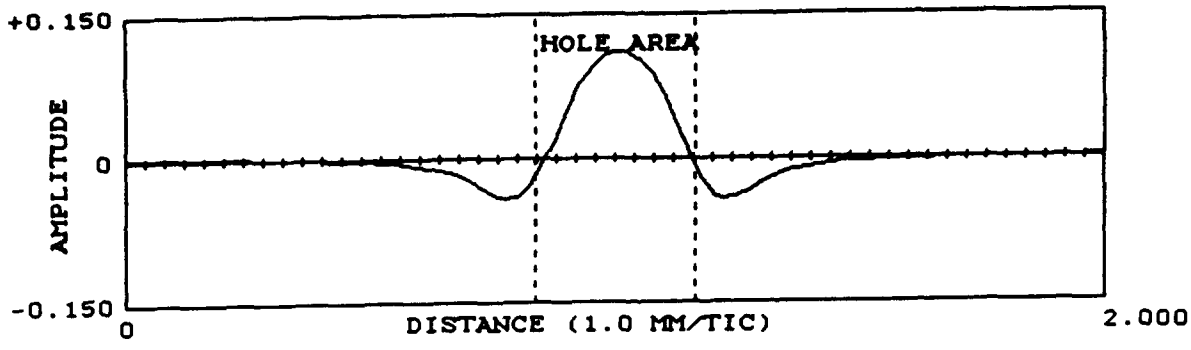


**FIGURE 29. TRANSVERSE MAGNETIC FIELD TRANSMITTED THROUGH 6.3 mm OF ALUMINUM SKIN WITH A 7.9 mm HOLE AT 10 kHz USING THE ELONGATED C-CORE PROBE.**

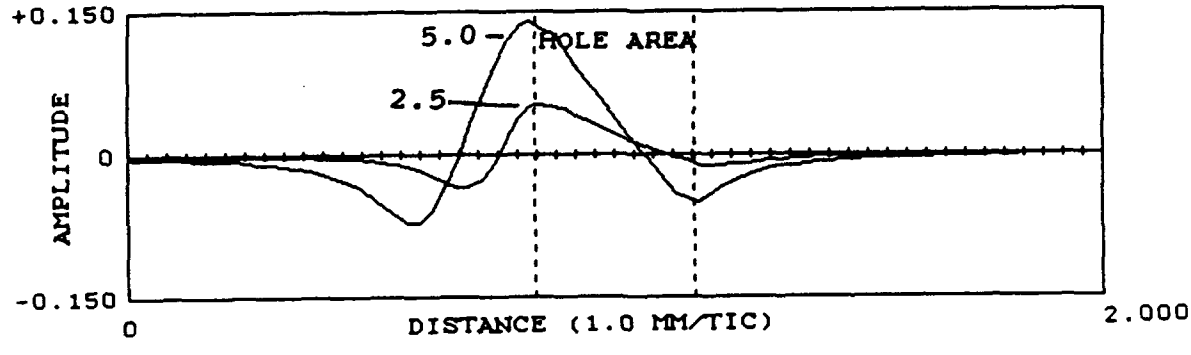


**FIGURE 30. TRANSVERSE MAGNETIC FIELD TRANSMITTED THROUGH 6.3 mm OF ALUMINUM SKIN WITH A 7.9 mm HOLE AND A 2.5 mm SLOT OR 5.0 mm SLOT AT 10 kHz USING THE ELONGATED C-CORE PROBE.**

had a large outer diameter (25 mm) which just touched the inside rim of the pot core, an inner diameter of 21 mm and a 2 mm height. This coil was representative of that portion of a drive coil windings which are near the rim of the core. The other coil had a smaller outer diameter (15 mm), an inner diameter (11 mm) which just touches the pot core center post and a 2 mm height. This coil was representative of that portion of a drive coil windings which are near the center post. The fields generated by each of these coils were measured when they were at a position flush with the core surface and at positions of increasing recession into the core. These measurements; when taken as a whole; demonstrate the effect of coil shape and placement within the core.

The field magnitudes generated by the large diameter coil were much greater than that of the smaller diameter coil (in proportion to the square of the diameter or coil area) as would be anticipated.

As a practical consideration, the drive coil needs to be slightly recessed (0.2 mm) in order to protect it from physical harm. However, in order to place sense elements nearer the probe center the drive coil(s) will need to be recessed up into the probe core a much larger distance (approximately 3 mm) to make room. A series of experiments were performed to determine if this would cause a significant reduction or alteration of sensitivity. Figure 31 shows the effect on the magnetic field distributions due to recessing the small drive coil from a position which is flush with the core face to recessed by 5 mm into the core. The magnetic field magnitude is only slightly reduced (8%) by recessing the drive coil. Recessing the drive coil also reduces the effect of the drive coil size on the field distribution. Recessing the drive coil makes the core shape the predominate factor in determining the field distribution. Notice on Figure 31 how when the drive coil is recessed the field magnitude nearer the outer rim of the core increased. This is due to the core acting as more of the field source without any direct field leakage from the drive coil. The general conclusion from this study is that we can fabricate probes with the sense coils placed under the drive coils without a loss of field penetration or sensitivity.

Another conclusion to be drawn from this study is that the most efficient drive coil shape is one which fully fills the core. This conclusion can be drawn from the fact that recessing the drive coil did not significantly reduce the fields generated, making the recessed portion of the coil as efficient as the flush portion. Previously, the probe for non-ferromagnetic fasteners was found to require a drive coil which fully fills the core. However, the optimum drive coil shape for probes for ferromagnetic fasteners was found to be a low profile drive coil located close to the core face. This discrepancy can be attributed to a combination of the sense coil placement and probe calibration which will not be used in future designs.

Additionally, since the ferrite core reduces the generated field dependence on coil placement within the core, it appears that any design using multiple drives for adjacent structure compensation will require the drives to be on opposite sides of a core wall. Concentric drive coils such as those used in this study, when placed between the same core walls, tend to have very similar field profiles at a typical second layer depth or at low

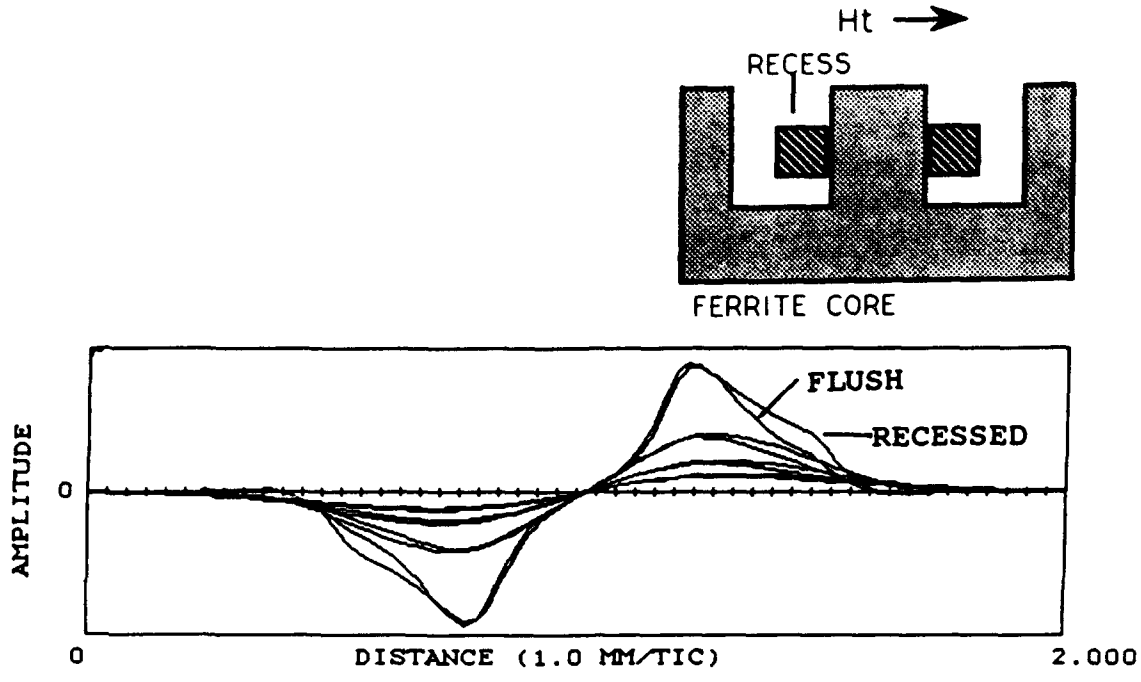


**FIGURE 31. TRANSVERSE MAGNETIC FIELDS GENERATED IN AIR AT DISTANCES OF 0, 2.5, 5.0, AND 7.5 mm FROM THE PROBE FACE WITH THE DRIVE COIL FLUSH WITH THE CORE FACE OR RECESSED 5.0 mm INTO THE CORE.**

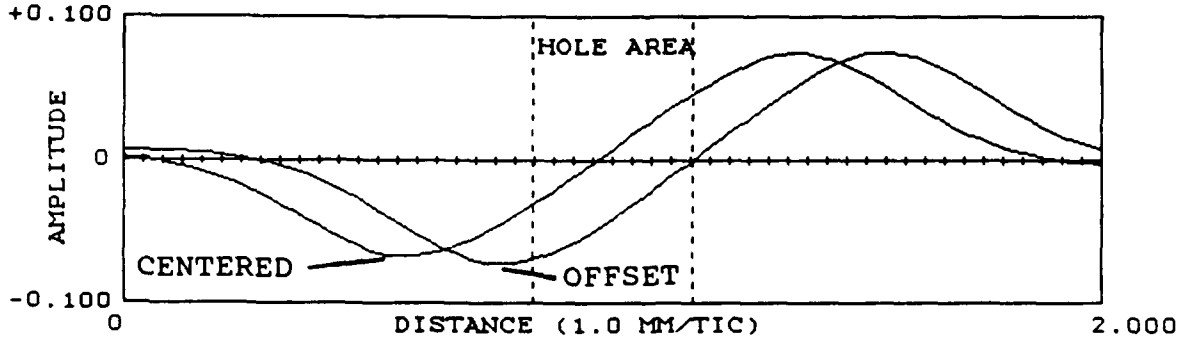


**FIGURE 32. TRANSVERSE MAGNETIC FIELDS TRANSMITTED THROUGH A 6.3 mm ALUMINUM SKIN WITH A 7.9 mm TITANIUM FASTENER INSTALLED FOR A CENTERED AND OFFSET PROBE.**

frequency. The near surface and high frequency field profiles will show some differences if the drive coil is of small height. A multiple drive concept using a small height drive could be used at high frequency for off-center and lift-off segregation.

### Multiple Drive Coils

To evaluate the use of multiple drive coils, a drive coil was placed around the outside of the core on the probes shown in Figures 19 and 20. A series of evaluations were made to determine the characteristics and sensitivity to edges, CUFs and off-center. The intent of these evaluations was to compare the effectivity of a multiple array versus a multiple drive or a combination of both concepts.

As already discussed, an array located outside of the core ( such as coil 5 of Figure 19) can be used to measure edge responses with only a small sensitivity to CUFs. A drive coil located around the outside of the core can also be used to accomplish the same result. Both approaches appear to be workable in a compensation routine. Using an outer drive coil is simpler and less expensive to construct. However, it appears that it may be easier to model the response of an outer array. With the addition of an outer array you measure the radial distribution of the perturbed fields. With an outer drive coil you measure the effect of radially displacing the drive currents. Each of the drive coils (inner & outer) will have a different depth dependence due to geometry and this effect needs to be incorporated in a compensation routine. Using an outer array and outer drive would provide significant information for compensation but may not be the simplest solution.

## 2.1.3 Probe Design Summary

An experimental database is now established to validate potential LFECA probe designs. The interaction of drive coil, sense coils and core as it pertains to detecting CUFs has been studied to the level required to design and construct optimum LFECA probes. They will incorporate design features which improve CUF sensitivity and reduce sensitivity to error signals. The greatest improvement in probe performance will be for the detection of CUFs through thick skinned or multilayered structures. Linear LFECA probe geometries were also shown to be strong candidates for crack detection.

## 2.2 Probe Motion - Offset

One of the possible methods proposed to improve CUF sensitivity and adjacent structure compensation was the use of probe offsetting. The general philosophy for this approach was to offset the probe from a centered position so that the peak in the eddy current distribution around the hole could be brought closer to the fastener hole wall. This would increase the current disrupted by a CUF and decrease the current disrupted by an adjacent structure. A larger diameter drive coil could also be used for greater penetration as well. This approach would require the probe to be moved in order to inspect completely around the hole. However, it was considered a way to significantly improve CUF sensitivity.

### Probe Offset - Nonferromagnetic Fasteners

Several experiments were performed to test the validity of probe offsetting and as an introduction to the effect of probe motion as an inspection parameter. Figure 32 shows the magnetic fields transmitted through a 6.3 mm aluminum skin for the case of a probe which is centered over the hole and one which is offset by 5 mm. This skin had a 7.9 mm titanium fastener installed in the hole. The fields are shown to directly translate with the probe movement. Although not shown in this figure, there is a large difference in the phase of the fields which are transmitted through the hole for the centered and offset cases. For this probe and thickness, offsetting the probe results in an approximate 50% increase in field magnitude within a region from the hole to 2.5 mm from the hole. This could be improved by using a larger coil. Also note that the field away from the hole would be reduced, resulting in a reduced sensitivity to adjacent structure. At a distance of 16 mm from the hole centerline, which would be a typical location for a structural edge to occur, the fields have dropped by approximately 50% as well. This is only true for one side of the hole and would require the probe to be moved in order to sensitively inspect the entire circumference of the hole. The advantage of this method is greater at shallower depths and high frequencies. This method could be incorporated into the probe design and used for each hole to be inspected or could be used as an additional inspection procedure to verify and help to determine the size of CUFs.

### Probe Offset - Ferromagnetic Fastener

Offsetting the probe with a steel ferromagnetic fastener installed results in a considerably different result. Figure 33 shows the magnetic fields transmitted through a 6.3 mm aluminum skin with a 7.9 mm steel fastener installed. Two cases are shown one in which the probe is centered over the hole and one in which the probe has been offset. There is only a small (15%) increase in the fields near the fastener and a slight decrease in the fields which would interact with adjacent structure. This is to small of an advantage to make an offset approach attractive.

The steel fastener acts as an effective extension of the probes center post and dominates the determination of the fields near the fastener. If a coil with a large inner and outer diameter is used then an advantageous offset effect can be observed. Figure 34 shows a scan of the magnetic fields through a 6.3 mm aluminum skin with a 7.9 mm steel fastener installed for a large probe which is centered and offset. An increase of 30% in field magnitude near the fastener is shown for the offset case. The limiting factor for this approach on steel fasteners is going to be a trade-off between an improved CUF sensitivity and increased fastener related error signals. This method could be implemented using probes designed to normally be used on larger steel fasteners.

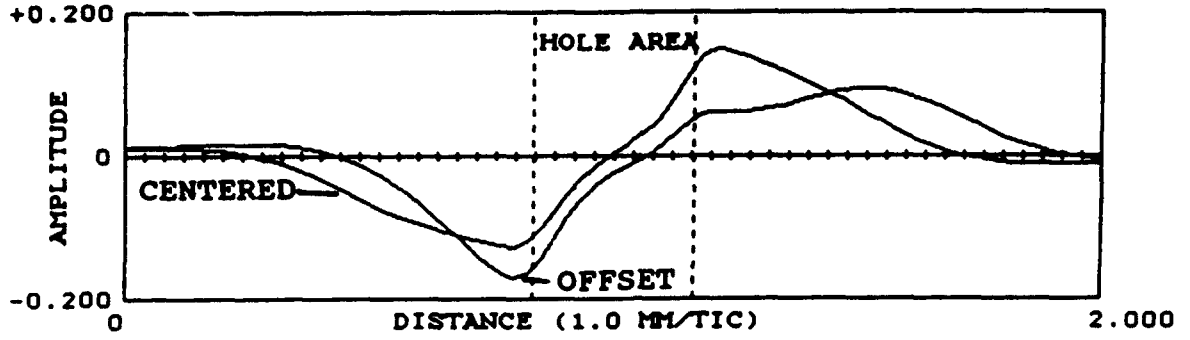


**FIGURE 33. TRANSVERSE MAGNETIC FIELDS TRANSMITTED THROUGH A 6.3 mm ALUMINUM SKIN WITH A 7.9 mm FERROMAGNETIC FASTENER INSTALLED FOR A CENTERED AND OFFSET PROBE.**

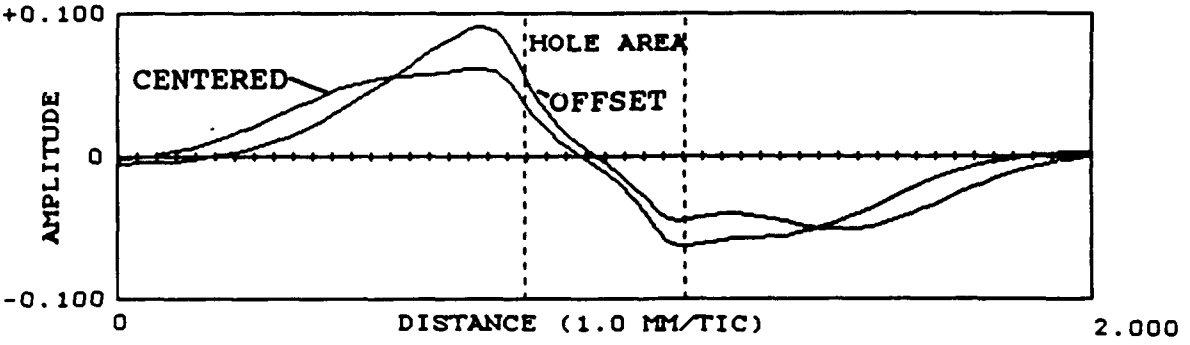


**FIGURE 34. SAME SET-UP AS FIGURE 33 BUT WITH A LARGER DIAMETER PROBE FOR A CENTERED AND OFFSET CONDITION.**

# SECTION 3

## TASK II - ALGORITHM DEVELOPMENT

The purpose of this task was to develop the algorithms required to remove or isolate interfering probe responses from CUF related responses. The overall objective being to realize an inspection which is simple to interpret and sensitive to CUFs. This task was mainly a software development effort in which compensation algorithms were devised, implemented and refined. The foundation for developing these algorithms was derived from the experimental evaluations from Task I. The algorithms that were developed use the unique features of the LFECA probe design, such as multiple drive coils and sense coil arrays, in combination with a multiparameter analysis method.

For the general case, the response generated by a LFECA probe when placed on a stener hole is not limited to just CUFs. The total response will be the result of several ctors in combination. Adjacent structure, probe placement, etc., will result in responses which interfere with interpreting whether or not a CUF is present. To a good approximation the total response can be thought of as being formed from a linear superposition of each effect. The following simple equation would be a mathematical representation of this statement:

(1) Probe Response = CUF + Off-center + Structure + Lift-off + Fastener

Each of these responses has a secondary effect on the other responses but this is usually a small effect which can be ignored. The most straightforward approach for discussing the compensation algorithms developed in this task is to discuss the approach taken for each of the individual effects. The following is a discussion for each of the major factors effecting the probe response.

### 3.1 Off-Center Response Compensation

The first thing that should be understood before discussing any response of a LFECA probe is that it is a relative response. The response observed on the LFECA system display is the result of a difference from a reference response. The reference response may be derived from many different sources but for the simplest case would derived from a known good fastener hole which is same as the unknown hole. Meaning the reference hole is surrounded by the same structure, is the same fastener material , etc. The reference hole may be derived from a standard or from a good hole on the inspected area. In any case, the response observed on the LFECA display is the result of a difference between the hole being inspected and the reference hole as shown in the following equation:

(2) Probe Response = Inspected Hole - Reference Hole

When a probe is placed on a hole which is the same as the reference hole the response will be a flat line (zero) response if the probe is placed centered over the hole. A probe which is placed off-center on the hole will result in a response. An off-center response has a characteristic spectral content, phase, and frequency dependence which can be used to identify it and remove it from the total response. Figure 35 shows a typical off-center response, the horizontal tick marks in the display indicate sense coil (1 to 16) and the vertical tick marks indicate response magnitude. The solid line is the real part (portion in-phase with the probe drive signal) and the dashed line is the imaginary part (portion 90 degrees out of phase with the probe's drive signal) of the complex response. The left side display shows the response at 9.8 kHz drive frequency and the right side display shows the response at 1.2 kHz. Both displays are with the inner drive coil driven (Figure 22 shows a sketch of the inner drive coil location). The response spatial spectra is primarily fundamental frequency ( looks like a single cycle of a sine wave) with typically 10% of second harmonic content. An off-center response can be accurately represented by using only the fundamental and second harmonic frequencies. The response magnitude is linearly proportional to the off-center distance and the spatial phase (position of sine wave along the horizontal axis) indicates off-center direction. Off-center also has a very consistent phase response (ratio of real /imaginary parts ) which is maintained over a wide range of off-center magnitude. There is also a linear scaling of the response with the inspection frequency.

At high frequencies (5 kHz and up) the probe response, when using the inner drive coil, will be limited to changes in the fastener hole and near surface. Adjacent structure will not be present in the response since the eddy currents generated by the probe will be limited to directly under the probe due to shielding by the aluminum skin. The probe's response will be sensitive to lift-off, off-center, first layer CUFs, and irregularities in the fastener/fastener hole. The following equation simply states the probe response at high frequency when using the inner drive coil:

(3) Probe Response = Lift-off + Off-center + Fastener Hole + 1st Layer CUF

Lift-off has a different phase response than off-center with the two responses being separated by 35 to 50 degrees, the exact angle depends on the particular probe. If you were to observe the responses on an impedance plane type display (complex plane) typical of eddy current instruments then off-center would be along the real (horizontal) axis and lift-off would be at a 35 to 50 degree angle with the real axis. Irregularities in the fastener/fastener hole such as oval countersinks and crooked holes will fall on the same phase angle as the off center response. The phase of a first layer CUF will depend on its depth into the aluminum skin.

The first step in compensating for off-center is to split the probe response into a lift-off and an off-center response. A simple trigonometric relationship can be used to separate the two responses by defining a lift-off phase and an off-center phase. The resulting off-center response is then analyzed using the known spectral characteristics of off-center to determine the magnitude of off-center present. The analysis also determines if

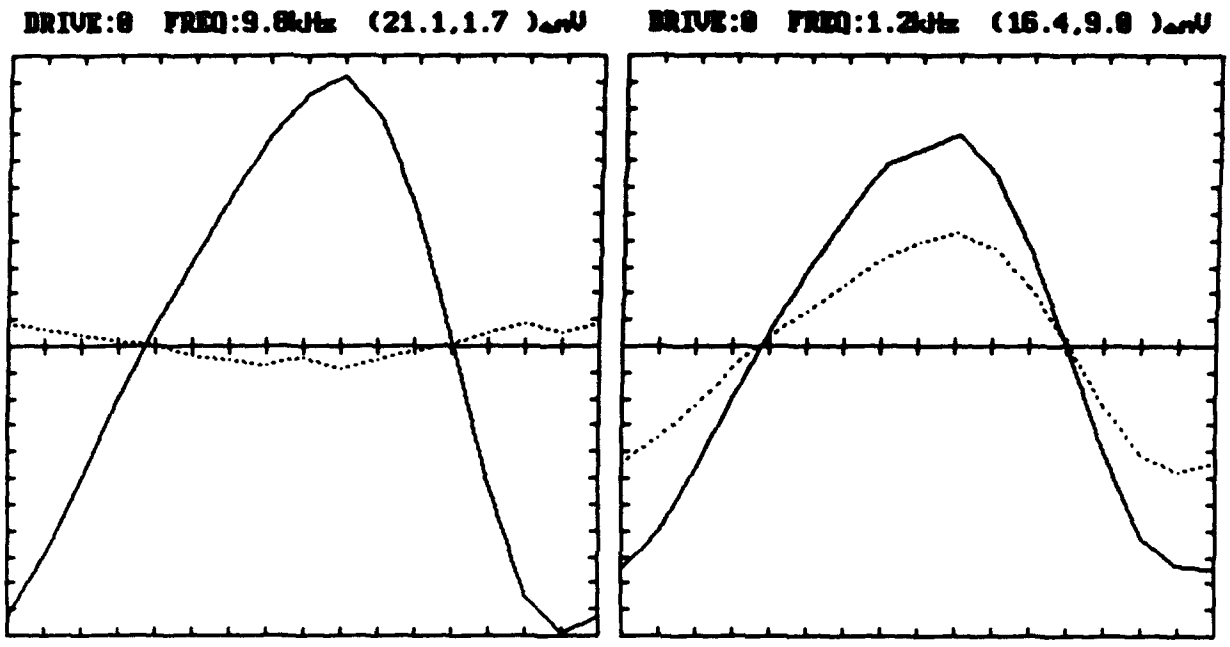


**FIGURE 35. TYPICAL OFF-CENTER RESPONSE.**

a first layer CUF is present and accounts for its presence when calculating the magnitude of off-center. A first layer CUF is distinguished by its sharp localized response (high harmonic content). The routine is also designed to detect the presence of multiple first layer CUFs. The resulting determination of off-center magnitude is then used to remove the off-center response from the high frequency response and to display an icon indicating off-center direction and magnitude. All of this occurs in real time so that the display shown during inspection has the off-center response removed.

To inspect into the second layer of a structure the high frequency drive signal is followed by a low frequency drive signal. This low frequency will reach down into the substructure to detect second layer CUFs. The off-center magnitude determined by the high frequency measurement is appropriately scaled and used to remove the off-center response from the low frequency measurement.

The accurate compensation for off-center using the above described scheme requires the accurate knowledge of the phase, spectra and frequency scaling of the off-center response. The phase is a very stable and consistent parameter which is simple to determine. The spectra and frequency scaling are more dependent on the application.

The spectra of the off-center response can be accurately approximated by using just the fundamental and second harmonic frequencies. The ratio of these harmonics is typically 10%, however, this ratio is not constant with off-center magnitude. In the range of normal off-center distances, the greater the off-center the smaller the percentage of second harmonic. If a single estimate for the ratio of second harmonic to fundamental frequency is used an error will result for certain ranges of off-center. To resolve this a non-linear relationship is estimated based on calibration data built into the system or an estimate can be made based on measurements at two off-center distances taken during the set-up procedure prior to an inspection.

The spectra of the off-center response is also dependent on the fastener hole size. A smaller hole results in a greater percentage of second harmonic. This ratio can be determined during set-up procedure or recalled from a set-up saved in a prior inspection. The scaling of the off-center response from high to low frequency is a stable parameter but needs to be determined as part of the set-up procedure or recalled from a prior set-up.

All of the above commentary on the requirement for determining frequency scaling and spectra scaling factors is to point out what is required for the routines to operate at their optimum. The error signals resulting from poor estimates for these scaling factors are easy to identify. They should not result in false calls but would more likely tend to mask small CUFs.

### 3.2 Lift-Off Response Compensation

Lift-off can be divided into two portions; straight lift-off and tilt; which are handled in different ways. Straight lift-off, due to variations in paint thickness for example, results in a dc shift of the probe response. Small amounts of straight lift-off typical of

paint thickness variations can be ignored. Since each sense coil has a slightly different coupling coefficient to the inspection area, each sense coil output is normalized to have the same output. The normalization factors are lift-off dependent so that large straight lift-off variations would require the probe to be renormalized to reduce noise due to inaccurate normalization. A different method for normalizing the probe output has been developed to compensate for large straight lift-off which basically adjusts the probe normalization based on the dc value of the probe response but has not been implemented to date. Typically straight lift-off has not been a concern.

Tilted lift-off is due to the probe being held at an angle with the aircraft skin's surface or the surface being not flat. The response shape for a tilt is very similar to an off-center response. Compensation for tilted lift-off is closely related to the off-center compensation. The high frequency response (using the inner drive coil ) is split into the lift-off and off-center phase responses during the off-center compensation routine. After recognizing and removing that portion of the lift-off response which is due to a first layer CUF, the lift-off response is appropriately scaled to remove lift-off from the low frequency response. Both off-center and lift-off responses are greater at high frequency than at low frequency so that any errors in the compensation routine are reduced when they are scaled down to the lower frequencies. Also, lift-off is generally a small effect at low frequency.

Currently a small hand held template is used to guide the probe to a centered condition over the fastener hole. The guide sits flat on the surface of the aircraft and will tilt if used on a curved surface. A simple modification of this template so that it can adjust to a curve surface has been devised. This would eliminate any tilted lift-off when inspecting curved surfaces which are the main cause for tilted lift-off.

Additionally, several simple design modifications have been devised which include special drive coils which would have sensitivity to only lift-off and no other effect. This would enable a totally independent measurement of lift-off for use in compensation. To date this does not appear to be necessary but remains an option.

### 3.3 Fastener Response Compensation

Within the category of fastener response we have grouped the responses due to the fastener hole as well as the fastener. Oval, crooked holes, and any feature which is not circularly symmetric will result in a response. Features due to the fastener hole will appear oriented in the same phase as an off-center response. They will appear as apparent noise after the off-center compensation routine has been performed. They will have the phase of a first layer near surface effect and generally are largely composed of second harmonic (for oval holes). They would tend to look like an error in the off-center compensation routine. Generally, they would not be mistaken for a first layer CUF but would tend to mask small first layer CUFs (<0.5 mm) from clear identification.

Responses due to the fastener are very small and can be ignored for titanium and non-ferromagnetic stainless steel fasteners. Due to their low electrical conductivity very

little current is generated in these fastener materials relative to the surrounding aluminum, so they have very little effect on any measurements. Aluminum fasteners which are protruding or crooked result in a response which has the same phase characteristics as a lift-off response. The routine used for lift-off compensation will handle any errors due to an aluminum fastener, no special compensation routine is required. The special drive coil designs referred to earlier which provide a separate measurement of lift-off would be useful for the case of segregating lift-off from fastener errors. However, this would generally not be of interest.

For the case of a ferromagnetic steel fastener, the fastener response has the same phase as a lift-off response. However, the magnitude of this response can become unmanageable when you use the standard LFECA probe design. When a modified LFECA probe design is used which limits the amount of eddy currents to be generated in the fastener head, fastener errors are reduced to a magnitude which can be handled by the lift-off compensation routine.

### 3.4 Structure Response Compensation

Within the category of structure response resides a broad range of features which will cause a response in the LFECA probe. The general categories for those features that were considered are thickness variations, first layer edges and second layer edges. An edge being any seam, splice or overlap that causes a discontinuity in the metallic structure near a fastener hole.

The simplest solution (at least partial solution) is to use a reference hole which has similar structural geometry. The reference hole can be derived from a standard, adjacent hole in the inspection area, or from a hole from a previously stored inspection. When a reference hole is used in this manner any displayed result will be due to a difference between the inspected hole and the reference hole. A response due to structural differences between holes is normally considerably less than the structural response. If the variation in structure is small no further compensation for structure need to be applied. However, this is generally not the case and further compensation is required.

A variety of compensation approaches were investigated with most depending on some new design feature of the probe. For example the use of multiple concentric sense coil arrays was evaluated. The general conclusion from these evaluations was that the use of a multiple drive coil scheme was the most straight forward approach.

In a multiple drive coil scheme, both an inner and an outer drive coil are present on the probe. The inner drive coil ( located on the probe center post) will generate a current distribution which will be sensitive to the fastener hole and CUFs but will also have some sensitivity to adjacent structure. The outer drive (located around the outside of the core) will generate a donut shaped current distribution which will be sensitive to the surrounding structure but will not be sensitive to the fastener hole or CUFs. The response with the outer drive coil energized is measured by the sense coil array as a measure of the adjacent

structure. For example, the full inspection would require the following responses to be measured:

1) High Frequency Response (10 kHz) - Inner Drive Coil Energized
2) Inspection Frequency Response (1 kHz) - Inner Drive Coil Energized
3) Inspection Frequency Response (1 kHz) - Outer Drive Coil Energized

Optional Step:

4) High Frequency Response (10 kHz) - Outer Drive Coil Energized

In step (1) the response that is used to remove lift-off, off-center and detect first layer CUFs is measured. In step (2) the response which will reach into the underlying substructure to detect second layer CUFs is measured. In step (3) the response used to remove adjacent structure response from the step (2) response is measured. Step (4) is an optional step that would be used to help identify the first and second layer edge responses.

The response measured when the outer drive coil is energized (step 3) will not require off-center compensation since there will be no sensitivity to off-center. However, lift-off is removed by appropriately scaling the lift-off response that was determined using the high frequency inner drive response (step 1). This is just a simple extension of the lift-off compensation routine to the outer drive coil response.

For simplicity, for the remainder of this discussion the response measured by the sense coil array when the inner drive coil is energized will be referred to as the "inner drive" response and the response measured by the sense coil array when the outer drive coil is energized will be referred to as the "outer drive" response.

After the lift-off and off-center compensation routines have been applied the inner drive response will contain structure and CUF responses and the outer drive response will contain only structure responses. The outer drive response is "appropriately scaled" and used to remove the structure response from the inner drive response. The inner drive response will then contain only CUF related responses. All other non-relevant responses will be removed.

The statement "appropriately scaled" made in the preceding paragraph is an oversimplification of the process required to remove structure response. There are several factors that must be considered in order to properly scale the outer drive response. The primary difficulty in scaling the inner and outer drive responses comes from the fact that the magnetic fields generated by the two coils have very different profiles. Their depth and radial dependence are different which is basically due to the difference in their diameters. This means that the scaling will be dependent on depth and radial location of an edge. These differences can be reduced by the proper selection of the drive coil geometry.

To overcome the depth dependence difference the outer drive response is split into a first and second layer edge responses. This is requires since the scaling will be different for the two portions of the response. This is a fairly straight forward process which is based on the difference in phase between a first and second layer edge. The difference in

scaling with radial distance requires a non-linear relationship between response magnitude and scaling be used. For a good number of application a linear approximation will be sufficient.

To aid in the structure compensation, an additional response using the outer drive at high frequency (step 4) has been evaluated. This response will be sensitive to only the first layer edge response and can be used to remove the first layer edge response from the lower frequency responses. It is not clear at this time if this step would be required but it does make the analysis more straightforward since it removes any ambiguity regarding the location of the first layer edge and provides an additional prediction of the edge responses.

All the above scaling factors are derived from standards, adjacent holes in the inspected area or from previously stored inspections. Using an adjacent hole results in the most accurate compensation.

After the structure response has been determined two possibilities were evaluated for the displaying of inspection results. The first possibility was to display the response with all non-relevant responses removed by compensation. This is the simplest to interpret but requires all compensation routines to work error free or at least the errors must be clearly distinguishable from CUFs and do not mask CUFs. The second possibility had two displays shown at the same time, the display on the left showing the inner drive response and the right side showing the outer drive response. Both responses are shown with lift-off and off-center removed. The outer drive response is also properly scaled to show the structure response in the same scale as the inner drive response. This type of display requires at little more interpretation but also provides more latitude for errors in the compensation routines. Some further evaluations will be required to resolve which approach will be best.

### 3.5 CUF Response and Sizing

The response remaining after the full compensation routine has been applied is ideally only due to CUFs. Typically some small amount of response due to errors or inadequacies in the compensation routine will remain. To resolve a CUF response from this error response an additional algorithm is applied. Two parameters can be used to identify a CUF, its phase versus depth dependence and it's spatial spectral content (shape) for a given drive frequency. The response due to a first layer CUFs are highly localized to just a few sense coils and have a phase close to that of an off-center response. The phase of an off-center response can be used as the reference phase for the first layer. As a CUF becomes larger (1 mm) there is a phase difference from the off-center response but for small CUFs (0.5 mm) the phase is very close to that of an off-center response. First layer CUFs are identified by their sharp response shape and located in the first layer by their phase and high frequency response.

Second layer CUFs (deeper than 2 mm from the surface) will not be detected in the high frequency (10 kHz) response used for lift-off and off-center compensation. Second layer CUFs will appear in the lower frequency response. The phase of the CUF response

will be shifted dependent on the frequency and depth of the CUF. The thicker the overlying skin the greater the phase difference between the CUF and an off-center response at a given frequency. For example, at an inspection frequency of 1.2 kHz the phase difference between an off-center and a second layer CUF under a 4.1 mm skin will be close to 90 degrees. The phase of the second layer CUF is approximately 90 degrees at one eddy current skin depth and can be estimated by the following equation:

(4) Second Layer CUF Phase = 90 degrees * 1st Layer Skin Thickness/Skin Depth

A routine is used in which the phase of the anticipated error response and the phase of the second layer CUF are input (this could be modified to be input in depth). This routine will then segregate the CUF response from the error response. The resulting response will essentially display the response from a depth slice in the part. A preliminary effort was made to make this an iterative process in which the routine will hunt for the CUF phase rather than requiring a phase to be preselected. Also the inclusion of a series of additional responses at different frequencies into the routine was considered. The idea being that they could be combined to give improved resolution with depth. This approach appears to be promising but requires too complex of a calibration routine to be of practical interest at present.

Estimating the size of a CUF can be most easily accomplished by simply observing the magnitude of the CUF response and correlating this magnitude with a reference standard or previously stored calibration table for this inspection application. The horizontal display axis could be adjusted to a non-linear scale reading in CUF length based on the calibration table. Estimates within 10% to 20% are reasonable expectations for this approach. However, using this approach will dependent on a prior knowledge of the relation between cross-sectional shape and radial length of the CUF. To overcome this limitation requires hat the systems depth resolution be substantially improved. This may be possible by using a multiple frequency measurement approach as outlined in the preceding paragraph.

# SECTION 4

# TASK III - DESIGN EVALUATION

In this task, the system design improvements developed in Tasks I and II are evaluated. A description of the effectiveness of these improvements is reported.

## 4.1 Validation Exercise

In order to evaluate the effectiveness of the LFECA system in a manner which would provide the most honest evaluation of it's abilities an independent evaluation was sought. Arraignments were made to perform the validation exercise established by the FAA at Sandia National Laboratories in Albuquerque, New Mexico. This exercise was performed at no cost to this program. The exercise was established as a blind test of the abilities of eddy current equipment to inspect a lap joint typical of a commercial airline fuselage. The exercise consists of the inspection of forty-three specimens with each specimen containing twenty fastener holes. Figure 36 shows a sketch of the specimen configuration. Specimens were constructed using two 1 mm thick 2024-t3 aluminum sheets which were fastened together with three rows of 4 mm diameter aluminum flush head rivets. Fatigue cracks were grown in the first layer of selected holes prior to riveting the panels. A range of crack sizes from 0.3 mm to 25 mm (a hole to hole crack) were grown within a $\pm$22 degree orientation ( 0 degrees being the direction from hole to hole). Holes with cracks on one and both sides of the hole were present. Specimens contained either none, a low, a medium or a high number of cracks. A total of 860 holes were inspected with 708 being unflawed holes.

The validation exercise contains only first layer CUFs, however, the large number of specimens to be inspected with real CUFs were thought to present an unique experience which would be instructive in the evaluation of the LFECA system.

A Sandia National Lab employee acted as the monitor, recording the location of each flaw indication according to the inspectors instructions. Additionally, either a high, medium, or low level of confidence was assigned by the operator for each flaw indication called. Confidence was recorded as a number from 1 to 3 with 3 being the highest confidence level.

To fully appreciate the detection requirements you need to consider the geometry of the cracks. The 100 degree countersink used for the flush head fasteners comes to a knife edge at the bottom of the first layer. This means that a crack will have a triangular shape until it extends beyond the countersink (>1.25 mm). The response of the LFECA system to a crack will be approximately proportional to the cross-sectional area of the crack. This means that for cracks less than 1.25 mm the CUF response will be proportional to the square of the crack length. There is an additional geometric factor which reduces the CUF response by another half. Also there will be some burring and

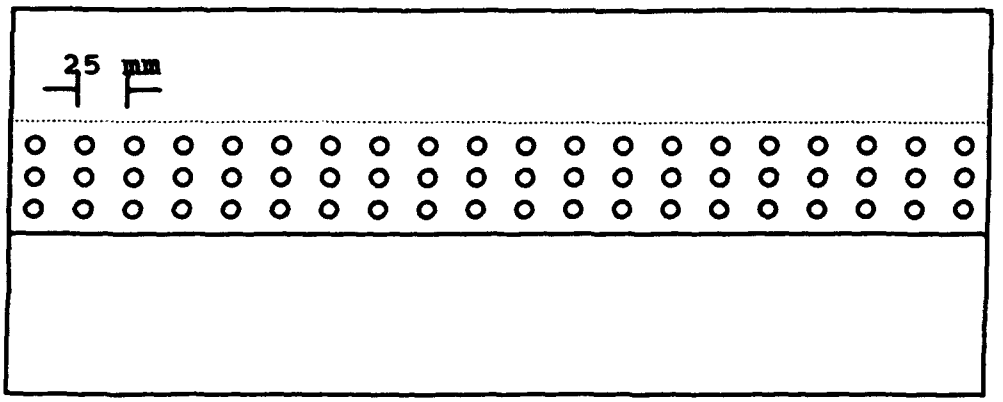


**FIGURE 36. SPECIMEN CONFIGURATION USED IN VALIDATION EXERCISE.**

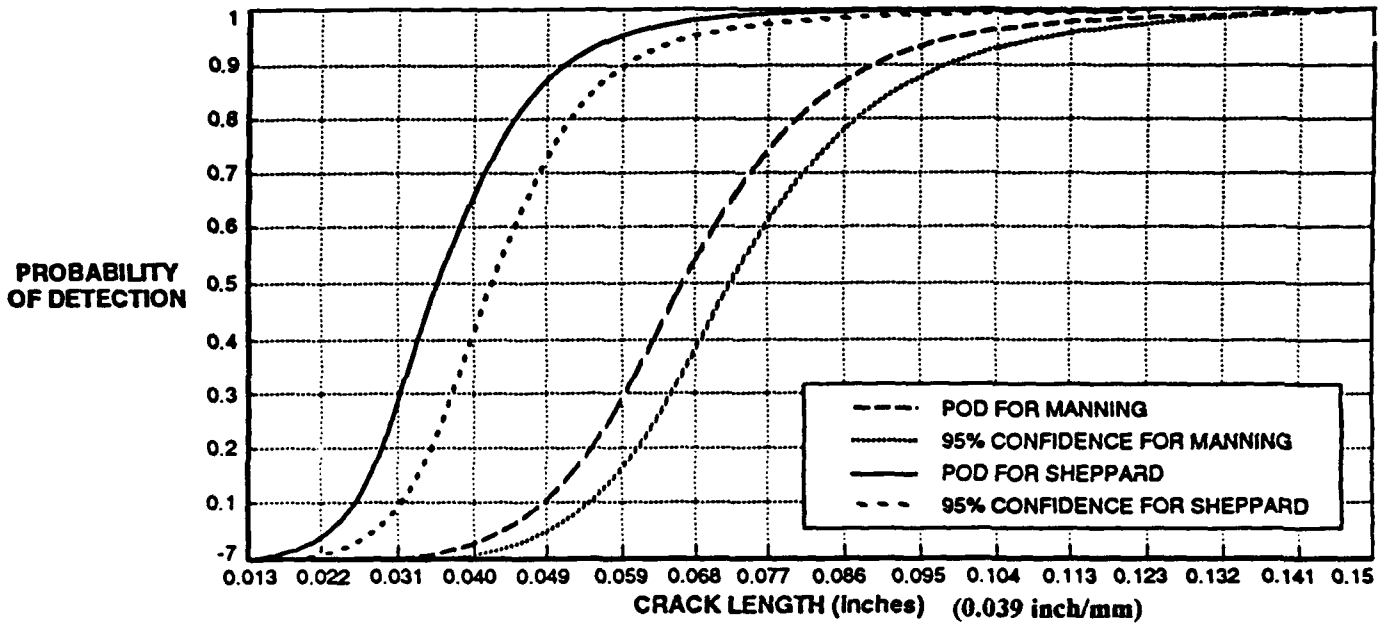


**SECOND EXERCISE**
EXPERIENCED OPERATOR - BILL SHEPPARD
PROBE DIAMETER - 16mm
CRACK STANDARD - 1 mm
COMPENSATION ALGORITHMS

**FIRST EXERCISE**
INEXPERIENCED OPERATOR - OWEN MANNING
PROBE DIAMETER - 18 mm
CRACK STANDARD - 2.5 mm
NO COMPENSATION ALGORITHMS

**FIGURE 37. PROBABILITY OF DETECTION (POD) CURVE FOR VALIDATION EXERCISES.**

fraying at the knife edge of the countersink which will add some noise level on the scale of a $\pm$0.25 mm.

The validation exercise was performed twice. The first time an inspector with only cursory training on the system was used. Also at that time no compensation routines were available in the system. After the first five panels were inspected, which essentially constituted the inspector's training program, no false calls were made and the majority of cracks over 1.25 mm were detected. These results were not indicative of the results to be expected using the system. However, the reasons for the less than optimum performance of the system/operator were very instructive.

Several factors effecting the performance were discovered and remedied. First the operator used a Boeing standard to set the display height for the inspection. The display was set to show a 2.5 mm slot on the Boeing standard at 80% of the screen height. The difficulty with this set-up is that a 2.5 mm slot will be more than 15 times greater than a 1 mm CUF. The result being that smaller CUFs would be missed by the operator. It was clearly apparent that this was the case after reviewing the stored inspection results with proper display settings. A large number of small CUFs that were easy to identify were passed over by the inspector. Two possible solutions were considered for this problem. A display with a non-linear horizontal axis could be used or the display could be set-up using a smaller CUF (1 mm). Setting up on a smaller CUF was the solution used for the next inspection. The file handling routine was also changed so that the display settings are now saved and recalled as part of the set-up for an inspection application.

Another difficulty experienced by the operator was interpreting the lift-off and off-center responses caused by the non-flat surfaces of the specimens. This was resolved by using the compensation routines for the next inspection. It was also discovered that the system did not store enough information about the inspection settings to fully recreate what the inspector had done. This was rather simple to fix.

For the second validation exercise an experienced operator of the LFECA system was used, all compensation routines were used, and the system was properly set-up. The result of this exercise was that all CUFs greater than 1 mm were detected with a level 3 confidence level with no level 3 false calls. Fifty percent of the 0.75 to 1 mm CUFs were detected with a confidence level of 3 or 2. Thirty-eight percent of the 0.5 to 0.75 mm CUFs were detected with a confidence level of 3 or 2. A total of six level 2 confidence level false calls were made. Of these six false calls, two were on holes without a CUF out of a total of 708 unflawed holes (0.28% false call rate). The four false calls on holes with a CUF were due to trying to interpret the presence of a small CUF on the opposite side from a large CUF.

Figures 37 shows the Probability of Detection (POD) curves from these exercises. POD and 95% confidence levels are shown for both times the validation exercise was performed. The results of the second validation exercise should be taken as the current status of the LFECA system capabilities. The first set of validation exercise results are

shown only to indicate the improvement in performance achieved by implementing some of the design improvements developed in this program.

The most difficult situation for detecting a CUF was when there was a small CUF on the opposite side from a large CUF. Small errors in the off-center compensation routine caused by the large CUF would tend to mask a smaller CUF located on the opposite side of the hole. Some minor adjustments in the compensation routines are being considered to correct this problem.

The probe used for this exercise was actually not the optimum probe for this inspection. If a smaller probe was constructed for this inspection application it would be reasonable to anticipate almost all 0.75 mm CUFs would be detected and a larger percentage of the 0.5 mm CUFs would be detected with high confidence.

## 4.2 Breadboard Design

A great deal of probe design concept evaluations are reported in section 2 of this report. Since no complete LFECA probes were constructed in this program, proposed design improvements will be evaluated based on the results of the breadboard design task experiments reported in section 2. The majority of experiments involved measurements which can be related back to the original LFECA probe designs for which the detection capabilities have been documented. Laboratory experiments have shown the detection limit for the original LFECA probe design was a 2.5 mm CUF located in a 6.4 mm thick aluminum second layer under a 6.4 mm thick aluminum skin.

The primary limitation of the original LFECA probe design was found to be the conflicting design requirements for a probe required to inspect deep into a structure. The original design would require the probe core diameter to increase for increased penetration depth. This requirement would also force the sense coils out further from the fastener hole as the core diameter increased. From the results of the experiments performed in this program it would be advantageous to increase the sense coil size and retain them closer to the fastener hole. New designs based on this approach will have better sensitivity to CUFs and a reduced sensitivity to adjacent structure. Several designs based on this approach are to be constructed for future LFECA systems. Based on the experimental evaluations a 50% sensitivity increase from the original design is anticipated for the new designs. Further evaluations on the detection of deep flaws and the generation of a CUF sensitivity versus depth chart for CUFs needs to be established with these new probes.

As a by product of the evaluations performed in this program it has become apparent that a significant improvement in performance could be achieved by improving the LFECA system's electronics. This effort was outside of the scope of this project but the potential for improvement and the design solutions were made apparent by the efforts in this program. Changes in the drive circuitry, probe cable, and input circuitry could be simply implemented resulting in a clear improvement in performance.

## 4.3 Algorithm Development

Section 3 contains a significant amount of analysis on the algorithm designs. The validation exercise and evaluations on test specimens in the laboratory have pointed out the strengths and weaknesses in the compensation routines implemented in this program. The routines for off-center and lift-off compensation will be further refined based of these evaluations. These routines appear to work quite well and are very effective in simplifying and speeding the inspection. The routines for structural compensation have shown to be very good at isolating and identifying the structural response which enables the operator to accurately interpret inspection results. However, they do require a higher degree of inspector skill/understanding to be accurately interpreted in certain cases. With further refinement and experience using these routines they could be made to be more generic and transparent to the operator. Implementing a nonlinear display scale which would be linear with CUF size would simplify CUF sizing. A modification of the display to convert response phase into CUF depth would also be a straight forward and helpful improvement.

# SECTION 5

# CONCLUSIONS

The objective of this program was to design an eddy current inspection system to detect CUFs in the second layer of fastened aluminum aircraft structures without requiring the removal of fasteners. Northrop's LFECA system was used as a baseline system for which design improvements were developed to improve second layer CUF detection capability.

A wealth of information was developed in the program on LFECA probe design. The following is a list of some potential design solutions and factors effecting probe design that were evaluated:

- Effect of driving frequency, CUF depth and size on the three dimensional fields generated by a CUF. Similar experiments also determined these relationships for the case of an off-centered probe, structural edges, and ferromagnetic fasteners.
- Potential variations in sense coil design such as coil placement, field component sensed (sense coil orientation), and multiple sense coil arrays were evaluated. All were evaluated for their potential for improving CUF sensitivity and improving the ability to segregate CUF responses from structural feature responses.
- The shape and size of the probe core were evaluated. The majority of emphasis being placed on the evaluation of circular array probe shapes due to the circular symmetry of the CUF inspection. However, several linear variations were investigated with very promising results.
- Drive coil shape and size, and multiple drive coil arrangements were investigated for the effect on CUF and structural feature response.

The result of these evaluations is a vast database of LFECA probe design knowledge from which new LFECA probe designs can be constructed with greatly improved performance for a range of applications. Improvements in both the CUF detection sensitivity , detection depth, and independence from complex structure can be achieved. A 50 to 100 percent improvement in sensitivity is predicted for new probe designs based on this program.

In the algorithm development task, software algorithms were developed to isolate and identify CUF responses from structural features. Compensation algorithms were developed for probe off-center, lift-off, fastener features, and structural edges. These algorithms used the unique features of the LFECA probe design, such as multiple drive coils and sense coil arrays, in combination with a multiparameter analysis method. Evaluations of these algorithms demonstrated their ability to improve inspection speed and reliability. The need for accurate centering of the probe over a fastener hole was minimized and structure effects were segregated from CUF responses to simplify inspection interpretation.

An evaluation of CUF detection reliability was conducted in an independently monitored exercise at the FAA Aging Aircraft NDI Validation Center at Sandia National Laboratories. These exercises were not supported by this program. However, the results of these exercises were used to optimize and validate the inspection procedures and algorithms developed in this program. These exercises demonstrated the improvement in CUF sensitivity and reliability achieved by implementing the compensation algorithms developed in this program. Figure 37 shows the POD curves generated for these exercises in which all CUFs 1 mm or greater were detected without false calls.

A great potential for further improvement in crack detection capability for the LFECA system was indicated by the following program results:

- LFECA probe design evaluations showed that the greatest potential for sensitivity improvement would be for the detection of CUFs under skins greater than 5 mm thick. Implementing and extending the results of these evaluations could dramatically improve crack inspection capability in thick multilayer structures.
- Alternate probe geometries were evaluated which would be attractive candidates for implementation in a corrosion or general crack detection system. For example implementing a linear LFECA probe design would extend the system's inspection capabilities to crack detection in bulkhead substructure.
- The use of probe motion was shown to improve CUF sensitivity. Implementation of a LFECA system with automated motion and imaging capability could be developed. This would increase inspection rates and sensitivity while also simplifying the interpretation of complex structure inspections.

In conclusion, this program was successful in demonstrating potential design options which would result in immediate improvement and forms the foundation for future improvements in CUF detection capability for complex aircraft substructures.

## REFERENCES


1. Hill, Brian and Sheppard, William, "Detecting Second-Layer Fatigue Cracks Under Installed Skins and Fasteners With Low-Frequency Eddy Current Array", Materials Evaluation, Vol. 50, Number 12, 1992, pg. 1398-1405.

2. Mih, David, "Improved Low Frequency Eddy Current Inspection For Cracks Under Installed Fasteners", Final Report, AFWAL-TR-80-4150, October 1980.

3. Bell, David, "Manufacturing Technology For Advanced Second Layer NDE System Producibility", Final Report, 1984.

4. Harrington, Roger, Time- Harmonic Electromagnetic Fields, 1987, pg. 53.

5. Spencer, Floyd, "Reliability Assessment at Airline Inspection Facilities Vol. II: Protocol For An Eddy Current Inspection Reliability Experiment", Final Report, DOT/FAA/CT-19/12, Federal Aviation Administration, May 1993.

6. Berens, A.P., Hovey, P.W., "Evaluation OF NDE Reliability Characterization", AFWAL-TR-81-4160, Vol. 1, Final Report, Dec. 1981.

7. Difference, D.M., MATHCAD Treasury of Statistics, Vol. II, Mathsoft Inc., 1993.

8. Spencer, Floyd, "Reliability Assessment at Airline Inspection Facilities, Vol. I A Generic Protocol for Inspection Reliability Experiments", Final Report, DOT/FAA/CT-92/12, I, Federal Aviation Administration, March 1993.